Steric effects in multiphoton excitation

Constantin Mainos
Laboratoire de Physique des Lasers, Université Paris-Nord, Avenue J. B. Clément, 93430 Villetaneuse, France
(Received 4 April 1994)

The effect of the spatial arrangement of a molecular internuclear axis and its plane of rotation in the multiphoton nonresonant excitation process is investigated. We consider diatomic or symmetric-top molecules; the internuclear axis is regarded to be fixed in space during the excitation time interval. Steric conditions preparing the initial angular distribution of the internuclear axis in the excited state are obtained, both for resolved and unresolved magnetic levels and for linearly or circularly polarized incident radiation. The intensities of individual rotational lines or rotational branches are obtained after averaging over all spatial orientations.

PACS number(s): 33.80.Rv, 33.70.−w

I. INTRODUCTION

Experiments have investigated in the past the possibility of orienting diatomic or symmetric-top molecules [1,2]. In principle, orientation for the molecular system involves both the net helicity of the angular momentum vector as well as the orientation of the internuclear axis. In particular, orientation for the internuclear axis in a selected rotational level has been obtained for the first time with NO molecules by exploiting the permanent electric dipole of this molecule in conjunction with the Stark effect and using strong hexapole electric fields [3]. The ground-state-oriented molecules then reacted with O_3 molecules and the reactivity showed a strong dependence on the orientation of the NO molecule.

Although an extensive investigation has been carried out in the past for orientation and alignment effects related to the angular momentum [4], as well as for rotational line strengths in multiphoton excitation [5], the relative lack of theoretical and experimental results concerning the orientation and alignment of the internuclear axis in the excited state is singular. This distinction probably emerges from the fact that, instead of the angular momentum vector for which the orientation remains fixed in space, the internuclear axis of the molecule constantly precesses and thus a fixed orientation in space cannot be attributed in a similar "direct manner."

A thorough understanding of the orientation of the internuclear axis in the excited neutral state is required since this topic is involved in a large number of experiments, i.e., this can be used in conjunction with resonant multiphoton ionization data for interpreting the angle-resolved photoelectron experiments given that the photoelectron intensities, as well as their angular distribution, are both sensible in the orientation of the internuclear axis in the intermediate excited state. A number of characteristics or properties, joined in sequence with the excited intermediate molecular state, may be studied. The oriented molecules in the neutral excited state can subsequently react with an atomic, molecular, or laser beam and furnish detailed information on the angular dependence of the reactivity, photodissociation, or photoionization of this state. A well-prepared selected state is a crucial parameter for the analysis and understanding of the dynamics of the above processes. In particular, the knowledge of the relative population between rotational and vibrational levels as well as the relative orientation of the molecular system with respect to the polarization vector of the incident radiation are explicitly required. Finally, it is worth pointing out that elucidation of chemical reactions on a molecular level is a major focus of the modern physical chemistry and this necessitates well-prepared oriented molecules both in their angular momentum as well in their internuclear axis. In such circumstances the spatial arrangement of the molecule in the excited state needs to be a controlled parameter.

The preparation of oriented molecules in an excited neutral state by optical methods is particularly attractive if the excitation process involves the absorption of more than one photon. This is due to the fact that, now, the angular momentum of the absorbed photons transfers an increasing anisotropy to the molecule. The molecule is not subject to strong hexapole electric fields and, moreover, it is not necessary to be restricted only to ground-state molecules possessing a permanent electric dipole.

In this work we consider the orientation dependence of a diatomic or symmetric-top molecule in the n-photon nonresonant excitation process. The excitation time interval being very short compared to a single molecular vibration or rotation the orientation of the internuclear axis is regarded as fixed in space during the excitation process. Due to the orientation dependence of the excitation process, a selection both for the internuclear axis as well as for the plane of molecular rotation takes place and an enhanced angular distribution for the initial orientation of the internuclear axis in the excited state is obtained. It is worth remarking that the alignment or orientation communicated to the molecular excited state cannot be lost by simple molecular rotation. We have only particular cases where the molecular excited state possesses a spherical angular distribution, i.e., $J_f = \frac{1}{2}$ unresolved M levels with linear polarization or states which can be depolarized by collisional relaxation before being further excited. In general, further excitation involves an

anisotropic initial state and this state is shown to carry an enhanced anisotropy if it is prepared by multiphoton excitation. Rotational line strengths of individual rotational lines which describe relative population appear as particular cases after averaging over all orientations for the molecular system.

II. THE ORIENTATION AND TRANSITION PATH DEPENDENCE IN THE n-PHOTON EXCITATION PROCESS

In this work we investigate the spatial arrangement of a diatomic or symmetric-top molecule in a multiphoton excitation. The involved electronic states are assumed to be well described by Hund's case (a) or case (b) electronic coupling and the multiplicity of the transition may be $2S+1$. To this extent, any of the coupling case sequences (CCS's) a-a, a-b, b-a, or b-b will be treated. Here we will consider the multiphoton process with n-identical photons of angular frequency ω and a polarization vector $\mathbf{e}_p$; the index p will stand for linearly ($p=0$), right ($+1$), or left (-1) circularly polarized light. Finally we will be concerned exclusively with the case of a dilute gas or with any system fulfilling collision-free conditions. Thus relaxation effects changing the angular momentum will be neglected.

We note by $|g\rangle$ the ground state of the molecule and by $|f\rangle$ the final excited state. The probability of the n-photon absorption may be deduced from the work of Bebb and Gold, who developed a perturbation theory for the multiphoton ionization of atoms. They obtain [6]

$$\mathcal{P}_{gf}^{(n)}=2\pi(2\pi aF\omega)^n\delta(\omega_{|g\rangle,|f\rangle})S_{gf}^{(n)} \tag{1a}$$

with $S_{gf}^{(n)}$, the rotational line strength, given by

$$S_{gf}^{(n)}=\sum_{M_g M_f}\left|\sum_{|i_{n-1}\rangle,\ldots,|i_1\rangle}\frac{\langle f|\mathbf{e}_p\cdot\boldsymbol{\mu}|i_{n-1}\rangle\langle i_{n-1}|\mathbf{e}_p\cdot\boldsymbol{\mu}|i_{n-2}\rangle\cdots\langle i_1|\mathbf{e}_p\cdot\boldsymbol{\mu}|g\rangle}{[\omega_{|g\rangle,|i_{n-1}\rangle}-(n-1)\omega]\cdots[\omega_{|g\rangle,|i_1\rangle}-\omega]}\right|^2 \tag{1b}$$

and F being the photon flux. The constant a is the fine-structure constant and ω is the angular frequency of each photon in the laser beam. The δ function takes account of the exact resonance between the n-photon energy and the energy difference between the ground and the final state. In what follows we consider the expression given in Eq. (1b) as the n-photon excitation probability. In this equation, $\boldsymbol{\mu}$ is the electric dipole moment operator of the molecule and the intermediate states $|i_1\rangle,\ldots,|i_{n-1}\rangle$ are assumed far from any exact resonance with any intermediate number of photons. Therefore, damping constants governing the decay of any intermediate state have been dropped from the energy denominator.

In the adiabatic approximation, we may separate the rotational from the electronic-vibrational variables by writing $|i\rangle=|i'\rangle|i''\rangle$ for all molecular wave functions of the involved states [7,8], where $|i'\rangle$ stands for the vibrational part and $|i''\rangle$ is the rotational wave function. Furthermore, the electric dipole component $\mu_p=\mathbf{e}_p\cdot\boldsymbol{\mu}$ may be transformed from the laboratory fixed frame (LFF) to the molecule fixed frame (MFF) in order to introduce the matrix elements of the electric dipole operator taken exclusively in the MFF. We have for each absorbed photon the following transformation: $\mu_p=\sum_q\mathcal{D}_{p,q}^{(1)*}(\alpha\beta\gamma)\tilde{\mu}_q$, with α, β, and γ the Euler angles of the MFF with respect to the LFF [9]. The tilde indicates that the electric dipole component is defined in the MFF.

Nevertheless, far from any exact resonance with an intermediate number of photons we may write the approximation $\omega_{|g\rangle,|i\rangle}\simeq\omega_{|g'\rangle,|i\rangle}$, since in this case we can neglect the rotational contribution. This may be done for all intermediate states and will permit one to perform the closure relation for all nonresonant intermediate rotational states, namely, $\sum_{|i''\rangle}|i''\rangle\langle i''|=1$.

Following the preceding discussion and developing the square conjugate of Eq. (1b), we obtain, for the excitation probability,

$$S_{gf}^{(n)}=\sum_{M_g,M_f}\left[\sum_{q_1,\ldots,q_n}\sum_{q_1',\ldots,q_n'}(S_{gf})_{q_1\cdots q_n}^{q_1'\cdots q_n'}\mathcal{V}_{gf}(q_1\cdots q_n)\mathcal{V}_{gf}^*(q_1'\cdots q_n')\right], \tag{2}$$

where $\mathcal{V}_{gf}(q_1\cdots q_n)$ is the electronic-vibrational operator, which is defined by

$$\mathcal{V}_{gf}(q_1\cdots q_n)=\sum_{|i_1'\rangle,\ldots,|i_{n-1}'\rangle}\frac{\langle f'|\tilde{\mu}_{q_n}|i_{n-1}'\rangle\langle i_{n-1}'|\tilde{\mu}_{q_{n-1}}|i_{n-2}'\rangle\cdots\langle i_1'|\tilde{\mu}_{q_1}|g'\rangle}{[\omega_{|g'\rangle,|i_{n-1}'\rangle}-(n-1)\omega]\cdots[\omega_{|g'\rangle,|i_1'\rangle}-\omega]}. \tag{3}$$

This operator is now independent of rotational quantum numbers since its matrix elements are taken in the MFF.

The tensor $(S_{gf})_{q_1\cdots q_n}^{q_1'\cdots q_n'}$ contains the rotational dependence of the excitation process and casts into the expression

$$(S_{gf})_{q_1\cdots q_n}^{q_1'\cdots q_n'}=\langle g''|\mathcal{D}_{p,q_1'}^{(1)}\cdots\mathcal{D}_{p,q_n'}^{(1)}|f''\rangle\langle f''|\mathcal{D}_{p,q_n}^{(1)*}\cdots\mathcal{D}_{p,q_1}^{(1)*}|g''\rangle$$
$$=\int_{\alpha=0}^{2\pi}\int_{\beta=0}^{\pi}\int_{\gamma=0}^{2\pi}\int_{\alpha'=0}^{2\pi}\int_{\beta'=0}^{\pi}\int_{\gamma'=0}^{2\pi}d\alpha\sin(\beta)d\beta\,d\gamma\,d\alpha'\sin(\beta')d\beta'd\gamma'g''^{*}(\alpha'\beta'\gamma')$$
$$\times\mathcal{D}_{p,q_1'}^{(1)}(\alpha'\beta'\gamma')\cdots\mathcal{D}_{p,q_n'}^{(1)}(\alpha'\beta'\gamma')f''(\alpha'\beta'\gamma')$$
$$\times f''^{*}(\alpha\beta\gamma)\mathcal{D}_{p,q_n}^{(1)*}(\alpha\beta\gamma)\cdots\mathcal{D}_{p,q_1}^{(1)*}(\alpha\beta\gamma)g''(\alpha\beta\gamma)\,, \tag{4}$$

where $g''(\alpha\beta\gamma)$ and $f''(\alpha\beta\gamma)$ are the rotational wave functions for the ground and the final state, respectively, which depend on the Euler angles and their electronic coupling case [8,9]. At this stage, if one performs the summations involved in Eq. (4) one will obtain an averaged contribution from the internuclear-axis orientation. The averaging operation with the matrix elements will hide internuclear-axis orientation effects and will lead to the rotational line strengths measuring population effects. The well-known electric dipole selection rules $M_f-M_g=np$ and $\Lambda_f-\Lambda_g=Q_n=Q_n'=q_1+q_2+\cdots+q_n$, for any electronic coupling case, can then be obtained by this operation.

We can clearly neglect molecular precession during excitation since the corresponding coherence time (excitation time interval $\sim10^{-15}$ sec) is very short compared to the rotational period ($\sim10^{-11}$–10^{-10} sec). Furthermore, we may assume that there is no significant reorientation for the internuclear axis within the above coherence-time interval from the transfer of the photon angular momentum. In fact, it seems improper to assume that the internuclear axis and the plane of molecular rotation may be reoriented from the angular momentum of one or more absorbed photons within a time interval of 10^{-15} sec, and this for inertial reasons. What seems most plausible is that roughly only molecules having their internuclear axis and their plane of rotation favorably oriented for the final rotational state are "preferentially" excited. A deviation from this favorable configuration will carry only weak probability amplitude; the excitation of the outer electron in a state of different symmetry inducing a modification of the plane of rotation within a time interval of some molecular periods.

From the above considerations it is understood that terms with $\alpha'\beta'\gamma'\neq\alpha\beta\gamma$ will be dropped from Eq. (4). To this extent, the distribution of the angles α, β, and γ may roughly characterize both the orientation of the internuclear axis in the ground state prior to the n-photon excitation as well as the initial orientation in the excited state if the time duration of the laser pulse is sufficiently short compared to a molecular rotation.

In previous work has been shown [10a] that the tensor $(S_{gf})_{q_1\cdots q_n}^{q_1'\cdots q_n'}$ vanishes whenever a single q_i' is different from q_i and $i=1,\ldots,n$. This holds for any electronic coupling case for the states involved. It is seen also that for our probability description the angles α and γ, which represent azimuthal rotations about the polarization vector and the internuclear axis, involve phase factors and do not play any role. These angles are then redundant. In order to lighten the notation, the angles α, β, and γ will be omitted from the rotation matrices.

Then from Eq. (2) we may specify the internuclear axis orientation in the excitation process from the expression

$$S_{gf}^{(n)}=\tfrac{1}{2}\sum_{M_g,M_f}\int_{\beta=0}^{\pi}\sin(\beta)d\beta S(\beta)\,, \tag{5}$$

with

$$S(\beta)=\sum_{q_1,\ldots,q_n}|g''^{*}\mathcal{D}_{p,q_1}^{(1)}\cdots\mathcal{D}_{p,q_n}^{(1)}f''|^2$$
$$\times|\mathcal{V}_{gf}(q_1\cdots q_n)|^2\,. \tag{6}$$

This is the angular excitation probability for the internuclear axis [10(b)]. The only angle involved in the excitation probability is the angle β, which locates the internuclear axis with respect to the polarization vector of the incident radiation. This angle is easily defined from laser pulses having time duration short enough compared to the rotational period of the molecule.

For the development of Eq. (6) we proceed as follows. First, from the contraction formula of two rotation matrices and from the associativity of the product of the n rotation matrices it may be seen that the product of the n rotation matrices obeys a permutation property for the set $q_1\cdots q_n$ [11]. Therefore, it is convenient to classify the n summations over $q_1,\ldots,q_n$ of Eq. (6) in three distinct sums by writing $\sum q_1\cdots q_n=(\sum Q_n)[\sum\alpha(Q_n)][\sum\mathcal{P}_q(\alpha)]$. Then $Q_n=q_1+q_2+\cdots+q_n$ takes the integer values from $-n$ to n and the sum over the transition paths $\alpha(Q_n)$ takes account of the fact that for a fixed value of Q_n we may have multiple sets $(q_1\cdots q_n),\ldots,(q_1'\cdots q_n')$ for which the sums of the q elements are always Q_n. Finally, $\mathcal{P}_q(\alpha)$ will stand for the sum over all distinguishable permutations of the q elements inside the transition path $\alpha(Q_n)$. The above classification can be made clear from Table I in Appendix A. Note that the product of the n rotation matrices remains insensitive to the q permutation and thus commutes with the summation over $\mathcal{P}_q(\alpha)$.

The product $\mathcal{D}_{p,q_1}^{(1)}\cdots\mathcal{D}_{p,q_n}^{(1)}$ may be contracted by considering the first two elements and then contracting the obtained result with the third one. By successive operations we obtain the desired result, which is outlined briefly in Appendix A.

Then one must define the electronic coupling case for the rotational states involved. We shall first consider the

case sequence b-b since the case sequence a-a is only a particular case of the case sequence b-b. This will be obtained subsequently by setting $S=0$ since for singlet molecular states there is no way to distinguish case (a) and case (b) coupling. We then take as the rotational wave function for Hund's case (b) coupling the wave function [12]

$$|N\Lambda SJM\rangle=[(2J+1)(2S+1)]^{1/2}(2N+1)\begin{bmatrix} N & 0 & N \\ -\Lambda & 0 & \Lambda \end{bmatrix} \times \sum_{\Sigma,\Omega}\begin{bmatrix} S & 0 & S \\ -\Sigma & 0 & \Sigma \end{bmatrix} \times \begin{bmatrix} S & J & N \\ \Sigma & -\Omega & \Lambda \end{bmatrix} \mathcal{D}^{(J)*}_{M,\Omega}|S\Sigma\rangle \, . \tag{7}$$

In general, far from intermediate resonances more than one transition path may take place. Then it is of prior interest to consider first the explicit dependence of the angular excitation probability in the allowed transition paths and subsequently "average" over all these allowed possibilities.

From Eqs. (6) and (7) and Appendix A we obtain, for the angular distribution,

$$S(\beta)=\sum_{Q_n}\sum_{\alpha}[S(\beta)]^{Q_n}_{\alpha}\left\{\sum_{\mathcal{P}_q(\alpha)}|\mathcal{V}_{gf}(q_1\cdots q_n)|^2\right\} . \tag{8}$$

The tensor $[S(\beta)]^{Q_n}_{\alpha}$ has the form

$$[S(\beta)]^{Q_n}_{\alpha}=(2J_q+1)(2N_g+1)(2J_f+1)(2N_f+1) \times\left|\sum_k \beta_{k,np}B^{(n)}_k(\alpha)_{Q_n}\left\{\sum_{\Sigma}\begin{bmatrix} N_g & S & J_g \\ \Lambda_g & \Sigma & -\Lambda_g-\Sigma \end{bmatrix}\begin{bmatrix} N_f & S & J_f \\ \Lambda_f & \Sigma & -\Lambda_f-\Sigma \end{bmatrix}\mathcal{D}^{(J_f)}_{M_f,\Lambda_f+\Sigma}\mathcal{D}^{(k)}_{-np,-Q_n}\mathcal{D}^{(J_g)*}_{M_g,\Lambda_g+\Sigma}\right\}\right|^2 . \tag{9}$$

In Eq. (9) we have used the fact that the rotation matrices are independent of spin variables. $S=S_g=S_f$ is the total spin angular momentum and $2S+1$ the multiplicity of the transition. Finally, for clarity, in Eqs. (8) and (9) the transition path $\alpha(Q_n)$ has been abbreviated by α.

Contracting the rotation matrix elements of Eq. (9) and developing the square conjugate, we obtain

$$\begin{aligned}[S(\beta)]^{Q_n}_{\alpha}=&\sum_{l'm'\omega'}(-1)^{m'-\omega'}(2l'+1)(2J_f+1)(2N_f+1)(2J_g+1)(2N_g+1) \\ &\times\sum_{\tau\tau'\gamma}\sum_{J'_fJ''_f}\sum_{l''L}(2\tau+1)(2\tau'+1)(2L+1)(2l''+1)(2J'_f+1)(2J''_f+1) \\ &\times\begin{bmatrix} l'' & L & l' \\ m' & 0 & -m' \end{bmatrix}\begin{bmatrix} l'' & L & l' \\ \omega' & 0 & -\omega' \end{bmatrix}\begin{bmatrix} \tau & l' & N_g \\ -\gamma & \omega' & \Lambda_g \end{bmatrix}\begin{bmatrix} \tau' & l'' & N_g \\ -\gamma & \omega' & \Lambda_g \end{bmatrix} \\ &\times\Bigg[\sum_{kk'}\beta_{k,np}\beta_{k',np}B^{(n)}_k(\alpha)_{Q_n}B^{(n)}_{k'}(\alpha)_{Q_n} \\ &\quad\times\left\{\begin{bmatrix} J_g & k & J'_f \\ -M_g & -np & M_g+np \end{bmatrix}\begin{bmatrix} J'_f & l' & J_f \\ -M_g-np & m' & M_f \end{bmatrix}\right. \\ &\qquad\left.\times\begin{bmatrix} J_f & l'' & J''_f \\ -M_f & -m' & M_g+np \end{bmatrix}\begin{bmatrix} J''_f & k' & J_g \\ -M_g-np & np & M_g \end{bmatrix}\right\} \\ &\quad\times\begin{bmatrix} N_f & k & \tau \\ \Lambda_f & -Q_n & -\gamma \end{bmatrix}\begin{bmatrix} N_f & k' & \tau' \\ \Lambda_f & -Q_n & -\gamma \end{bmatrix}\begin{Bmatrix} N_f & k & \tau \\ J_f & J'_f & l' \\ S & J_g & N_g \end{Bmatrix} \\ &\quad\times\begin{Bmatrix} N_f & k' & \tau' \\ J_f & J''_f & l'' \\ S & J_g & N_g \end{Bmatrix}\Bigg]P_L(\cos\beta) \, . \end{aligned} \tag{10}$$

From the $3j$ symbols we see that only the $l'=0$ term (or alternatively the $l''=0$ term) satisfies the electric dipole selection rule $M_f-M_g=np$. In the above term only the $J_f'=J_f$ value is allowed and the remaining sum over the angular momenta $J_f''\neq J_f$ stands for contributions from adjacent rotational levels. Nevertheless, the $3j$ symbols show that all angular momenta J_f'' have the same projection as J_f both in the MFF and the LFF of reference. Also, it may be seen [13] that under exact resonance conditions and using an infinitely sharp laser beam appreciable contribution from adjacent rotational levels may appear only for $\Gamma>0.3\ \mathrm{cm}^{-1}$ and for the lowest rotational levels. This arises since allowed electric dipole transitions have natural linewidths of the order of $0.001\ \mathrm{cm}^{-1}$ and the rotational constants are not much smaller than $0.1\ \mathrm{cm}^{-1}$ [14]. Then, from angular momentum and energy considerations it follows that only the $J_f''=J_f'=J_f$ term needs to be considered in allowed electric dipole transitions.

On carrying out the calculus and grouping the different dependences of Eq. (10), after keeping only the electric dipole term, we obtain the explicit contribution from the transition path to the angular distribution. This is written

$$[S(\beta)]_\alpha^{\Delta\Lambda}=\sum_{L=0}^{2J_f}[\sigma_L]_\alpha^{\Delta\Lambda}P_L(\cos\beta)\ . \tag{11}$$

The tensor $[\sigma_L]_\alpha^{\Delta\Lambda}$ stands for the path orientation asymmetry (POA) tensor when the excitation process follows the transition path α. It is given by

$$[\sigma_L]_\alpha^{\Delta\Lambda}=\sum_{kk'}\beta_{k,np}\beta_{k',np}B_k^{(n)}(\alpha)_{Q_n}B_{k'}^{(n)}(\alpha)_{Q_n}\times\mathcal{M}_{kk'}^{(L)}(M)\Theta_{kk'}^{(L)}(\text{b-b})\ , \tag{12}$$

where $\mathcal{M}_{kk'}^{(L)}(M)$ is responsible for the asymmetry brought from the $M_f=M_g+np$ independent channel when the transferred angular momentum is k. The tensor $\mathcal{M}_{kk'}^{(L)}(M)$ is defined by

$$\mathcal{M}_{kk'}^{(L)}(M)=(2J_f+1)\begin{pmatrix}J_g & k & J_f\\ -M_g & -np & M_f\end{pmatrix}\times\begin{pmatrix}J_f & 0 & J_f\\ -M_f & 0 & M_f\end{pmatrix}\begin{pmatrix}J_f & L & J_f\\ -M_f & 0 & M_f\end{pmatrix}\times\begin{pmatrix}J_f & k' & J_g\\ -M_f & np & M_g\end{pmatrix}\ . \tag{13}$$

The letter M will stand for either M_g or M_f since they are univocal. Since the isotropic term of the excitation probability is responsible for population effects, the isotropic term $\mathcal{M}_{kk}^{(0)}(M)$ may be associated with the population weighting factor of the M channel when the transferred angular momentum is k. For the weighting factor of all M channels we then find $\sum_{M_g,M_f}\mathcal{M}_{kk}^{(0)}(M)=1/(2k+1)$.

The rotational line asymmetry (RLA) tensor $\Theta_{kk'}^{(L)}(\text{b-b})$ contains the b-b electronic coupling case sequence and is given by

$$\Theta_{kk'}^{(L)}(\text{b-b})=(2L+1)(2J_g+1)(2N_f+1)(2J_f+1)^2(2N_g+1)^2\begin{pmatrix}N_g & 0 & N_g\\ -\Lambda_g & 0 & \Lambda_g\end{pmatrix}\begin{pmatrix}N_f & k & N_g\\ \Lambda_f & -Q_n & -\Lambda_g\end{pmatrix}\times\begin{Bmatrix}N_f & k & N_g\\ J_f & J_f & 0\\ S & J_g & N_g\end{Bmatrix}\sum_{N_g'}(2N_g'+1)\begin{pmatrix}N_g' & L & N_g\\ -\Lambda_g & 0 & \Lambda_g\end{pmatrix}\begin{pmatrix}N_f & k' & N_g'\\ \Lambda_f & -Q_n & -\Lambda_g\end{pmatrix}\begin{Bmatrix}N_f & k' & N_g'\\ J_f & J_f & L\\ S & J_g & N_g\end{Bmatrix}\ . \tag{14}$$

For the remaining CCS the tensor $\Theta_{kk'}^{(L)}\mathcal{C}$ is given in Appendix B. It can be easily verified that the tensor component $\Theta_{kk'}^{(0)}\mathcal{C}$ is identical to the corresponding rotational line factor. If we set $S=0$ in Eq. (14) and replace everywhere N by J and Λ by Ω we obtain the case sequence a-a RLA tensor given in Appendix B.

From Eqs. (11), (12), and (14) we see that the excitation probability is nonvanishing only when $Q_n=q_1+q_2+\cdots+q_n=\Lambda_f-\Lambda_g=\Delta\Lambda$. The above selection rule will provide the allowed transition paths for the n-photon process. In fact, for the analytic expression of the angular distribution we need to define precisely the number of transition paths involved. From the MFF electric dipole components $\tilde{\mu}_{q_1},\tilde{\mu}_{q_2},\ldots,\tilde{\mu}_{q_n}$, associated with the n photons, the set $q_1,q_2,\ldots,q_n$ will constitute a transition path only if the above selection rule is satisfied; then from the 3^n sets only a limited number is allowed. These paths can be determined from n and $\Delta\Lambda$; for instance, in a $\Delta\Lambda=1$ three-photon transition there are only two allowed paths, namely, (001) and (1-11). It may be seen [15] that in general, the number of the allowed transition paths is given by $\alpha(n,\Delta\Lambda)=\mathrm{Int}[(n-|\Delta\Lambda|+2)/2]$. Then the angular distribution for the internuclear axis in the n-photon process simplifies to

$$S(\beta)=\sum_{\alpha=1}^{\alpha(n,\Delta\Lambda)}[S(\beta)]_\alpha^{\Delta\Lambda}|\mathcal{V}_{gf}(\alpha,\Delta\Lambda)|^2\ , \tag{15}$$

with

$$|\mathcal{V}_{gf}(\alpha,\Delta\Lambda)|^2=\sum_{\mathcal{P}_q(\alpha)}|\mathcal{V}_{gf}(q_1\cdots q_n)|^2 \tag{16}$$

and $\mathcal{P}_q(\alpha)$ standing for the sum over all distinguishable permutations of the individual MFF electric dipole components inside the transition path α.

The key formulas for our investigation are Eqs. (11) and (15). For a given electronic transition $\Delta\Lambda$ and a spin multiplicity $2S+1$ the angular distribution for the internuclear axis is expressed in terms of the allowed transi-

tion paths, while each transition path brings its own angular distribution. The electronic-vibrational contribution from the transition path α is condensed in the factor $|\mathcal{V}_{gf}(\alpha,\Delta\Lambda)|^2$. It is worth noting that the above contribution in the angular distribution emerges exclusively from the multiplicity of the composite angular momentum (CAM) allowed values and that of the allowed transition paths. This is involved in the tensor $B_k^{(n)}(\alpha)_{\Delta\Lambda}$, i.e., we observe that if a single transition path is dominant in the nonlinear process the whole electronic-vibrational contribution factors, we then obtain $S(\beta)\sim[S(\beta)]_\alpha^{\Delta\Lambda}$ [16].

III. THE ANGULAR DISTRIBUTION IN THE AVERAGED MULTIPHOTON ELECTRIC DIPOLE APPROACH

Orientation experiments are primarily concerned with the relative occupation probability of the different sublevels $M_f=M_g+np$ in the excited state. We shall therefore first consider the case of resolved magnetic levels where the polarized incident radiation is assumed in resonance with some rotational subline $N_gJ_gM_g\rightarrow N_fJ_fM_f$. From Eqs. (11) and (15) we obtain

$$S(M;\beta)=\sum_{L=0}^{2J_f}\sigma_L(M)P_L(\cos\beta)\ . \tag{17}$$

All the asymmetry brought to the molecular system from the oriented angular momenta is contained in the molecular orientation asymmetry (MOA) tensor $\sigma_L(M)$. This tensor is given by

$$\sigma_L(M)=\sum_{kk'}\beta_{k,np}\beta_{k',np}\mathcal{B}_{kk'}^{(n)}\mathcal{M}_{kk'}^{(L)}(M)\Theta_{kk'}^{(L)}\mathcal{C} \tag{18}$$

and the quantity $\mathcal{B}_{kk'}^{(n)}$ is the only quantity involving contribution from the allowed transition paths. We have

$$\mathcal{B}_{kk'}^{(n)}=\sum_\alpha B_k^{(n)}(\alpha)_{\Delta\Lambda}B_{k'}^{(n)}(\alpha)_{\Delta\Lambda}|\mathcal{V}_{gf}(\alpha,\Delta\Lambda)|^2\ . \tag{19}$$

By inspection of Eqs. (17)–(19) we observe that both for resolved and unresolved magnetic levels excitation with linearly polarized light will involve the quantity $\mathcal{B}_{kk'}^{(n)}$, which in turn requires the knowledge of the multiphoton-electronic-vibrational (MEV) parameters $|\mathcal{V}_{gf}(q_1\cdots q_n)|^2$ following Eqs. (16) and (3). Frequently the particular case is found where a single transition path dominates the transition, then the whole MEV-dependence factors from the excitation probability, and therefore the angular distribution can be explicitly determined [16]. In general, however, multiple transition paths are present and interact with more than one allowed CAM vector, in which situation the electronic-vibrational contribution should be taken into account. This can be done by keeping in mind that any intermediate number of photons is found out of resonance; then we may assume that the assembly of the allowed molecular states plays an equally important role for each individual MFF electric dipole component $\tilde{\mu}_q$. This might diverge only when the energy of an intermediate number of photons is found in exact resonance with some allowed molecular state.

Thus, in similar situations, we may assume that the involved MEV parameters contribute roughly equally to the nonresonant process. This also means that the excitation probability is insensitive to the order in which the individual MFF dipole components $\tilde{\mu}_q$ occur in the excitation process providing that they satisfy the selection rule $q_1+q_2+\cdots+q_n=\Delta\Lambda$.

In the averaged multiphoton electric dipole approach, the contribution from the electronic and vibrational structure is then condensed into the tensor

$$\overline{\mathcal{B}}_{kk'}^{(n)}=\sum_{\alpha=1}^{\alpha(n,\Delta\Lambda)}\mathcal{N}(\alpha)B_k^{(n)}(\alpha)_{\Delta\Lambda}B_{k'}^{(n)}(\alpha)_{\Delta\Lambda}\ , \tag{20}$$

whereas the MEV parameters factorize and thus have been dropped. The quantity $\mathcal{N}(\alpha)$ stands for the number of distinguishable permutations of the individual MFF dipole components in the transition path α and appears from the summation over $\mathcal{P}_q(\alpha)$ following Eqs. (16) and (19). It has the expression $\mathcal{N}(\alpha)=n!/[n(-1)!n(0)!n(1)!]$ and this coefficient may be seen as a transition path weighting factor; n is the number of photons and $n(q)$ is the number of q (-1,0, or 1) components in the transition path α. For instance, for the transition path (110) of a $\Delta\Lambda=2$ three-photon transition we obtain $n!=6$, $n(1)!=2$, $n(0)!=1$, and $n(-1)!=1$, which result in $\mathcal{N}(\alpha)=3$ and take into account the three distinguishable permutations (110), (101), and (011) for which $q_1+q_2+q_3$ always equals $\Delta\Lambda$.

Then, after inspection if Eqs. (18) and (20), if one defines the tensor

$$\overline{c}_{kk'}^{(n)}(p)=\beta_{k,np}\beta_{k',np}\overline{\mathcal{B}}_{kk'}^{(n)}\ , \tag{21}$$

one will obtain a simple expression for the MOA tensor $\overline{\sigma}_L(M)$, which is involved in Eq. (17). This tensor reduces to the simple form

$$\overline{\sigma}_L(M)=\sum_k\overline{c}_{kk'}^{(n)}(p)\mathcal{M}_{kk'}^{(L)}(M)\Theta_{kk'}^{(L)}\mathcal{C}\ . \tag{22}$$

The analysis and understanding of the $\overline{c}_{kk'}^{(n)}(p)$ tensor coefficient is made clear in Appendix A where numerical values are presented for up to seven photon processes. From this analysis we obtain the closure relation $\sum_{k=0}^{n}\overline{c}_{kk}^{(n)}(p)=1$, which holds for either linear or circular polarization. All off-diagonal terms of this tensor vanish and in Eq. (22) we have used the fact that $\overline{c}_{kk'}^{(n)}=\overline{c}_{kk}^{(n)}\delta_{kk'}$. For the particular case of circular polarization we obtain $\overline{c}_{kk}^{(n)}(1)=\overline{c}_{kk}^{(n)}(-1)=\delta_{k,n}$. The above tensor has assumed, for each CAM vector, an averaged contribution from the MEV parameters and this has been indicated by an overbar.

Finally, for numerical calculations and ease of comparison of the intensity distribution in the rotational branches, Eq. (17) is normalized to unity. In fact, if one averages the excitation probability $S(M;\beta)$ over all M values and β orientations and sums over all levels Λ_f,J_f,N_f, which may be attained from the ground level Λ_g,J_g,N_g, one will obtain, by virtue of angular momentum closure relations [17(a)] and the closure relation of the $\overline{c}_{kk}^{(n)}(p)$ tensor that this equals $2J_f+1$. Therefore, the

normalized expression of the angular distribution leads to

$$S(M;\beta)=S(M)\left\{1+\sum_{L=1}^{2J_f}\bar{\sigma}_{LO}(M)P_L(\cos\beta)\right\}, \quad (23)$$

where $\bar{\sigma}_{LO}(M)=\bar{\sigma}_L(M)/\bar{\sigma}_0(M)$ is the molecular orientation asymmetry parameter (MOAP) and $S(M)=\bar{\sigma}_0(M)/(2J_g+1)$ is the relative occupation probability for the M channel, which constitutes the amplitude for the angular distribution of the internuclear axis. We then observe that for resolved magnetic levels all the $2J_f+1$ components for the MOAP tensor are participating; the $L\neq 0$ components will contribute to the asymmetry of the angular distribution whereas the $L=0$ component will be responsible for population effects. The tensor $S(M)$ describing the relative occupation probability of the M_f magnetic level in the excited state casts into

$$S(M)=\frac{1}{2J_g+1}\sum_k \bar{c}_{kk}^{(n)}(p)\begin{pmatrix} J_g & k & J_f \\ M_g & np & -M_f \end{pmatrix}^2 \Theta_{kk}^{(0)}\mathcal{C}. \quad (24)$$

The angular distribution for the internuclear axis, given in Eq. (23), holds for any coupling case sequence. Note also that the above equation has a similar form as the differential cross section of the photoelectrons produced by incident polarized radiation in the electric dipole approximation. The coefficient $\bar{\sigma}_{LO}(M)$ is associated with the asymmetry parameter and β is the angle between the polarization vector and the direction of the photoelectron. However, for the complete description of such processes the continuum wave function of the final state, instead of the bound state, should be considered.

The angular distribution $S(M;\beta)$ may be seen either as the probability $S(M_g;\beta)$ of exciting oriented molecules or as the initial angular distribution $S(M_f;\beta)$ of the molecules having been selected from an isotropic ground state, these two pictures approaching equivalence for shorter and shorter laser pulses. A rotational blurring should appear for the angular distribution if the laser pulse duration is not sufficiently short compared to a molecular rotation.

In collision-free conditions the angular momentum J_g of the unperturbed molecule is fixed in space whereas the internuclear axis precesses about J_g with a rotational period typically on the order of 10^{-11}–10^{10} sec. We may assume without loss of generality that the incident radiation does not affect significantly the rotational motion of the internuclear axis and thus the precessional frequency remains constant. However, during the internuclear axis precession, all orientations for this axis do not present the same excitation probability; for instance, the projection of the space-fixed CAM vector [17(b)] on the internuclear axis is constantly modified. It may be seen that only some specific orientations enhance the excitation probability.

The most relevant feature emerges from the simple case where only the $M_f=\Omega_f$ (or $M_f=-\Omega_f$) sublevel is excited with linear polarization. In Fig. 1(a) we show the relative strength $S(M;\beta)$ for the allowed M channels in the $Q(\frac{9}{2})$ branch line of the NO $A\,^2\Sigma^+(b)\leftarrow X\,^2\Pi_{3/2}(a)$ two-photon transition. This distribution is plotted for linear polarization and we have assumed that the ground and the excited state are well described by Hund's case a and b rotational wave functions, respectively. Then we observe that, for the overall angular distribution $S(\beta)$, the channels $M_f=M_g=\pm\Omega_f$ and $M_f=M_g\pm J_f$ are determining. It is seen that selective excitation of the $M_f=\Omega_f=\frac{1}{2}$ sublevel clearly favors internuclear axes being oriented in the polarization vector direction; this specific orientation may be seen as the most plausible for which the angular momentum in the excited state presents a common projection $M_f=\Omega_f=\frac{1}{2}$ both on the LFF and MFF quantization axes. In contrast selective excitation of the $M_f=-\Omega_f=-\frac{1}{2}$ sublevel favors only internuclear axes antiparallel to the polarization vector. This selection holds for any rotational branch ΔJ and any number of photons n providing that only the $M_f=\pm\Omega_f$ sublevel is excited.

Thus selective excitation of these specific channels leads to strong steric effects since the number of excited molecules having their internuclear axis parallel and antiparallel to the polarization vector is not the same [17(c)]. Instead, for unresolved M levels (where all allowed M channels are excited simultaneously) the above steric effect is absent. This has been shown by the angular distribution $S(\beta)$, which involves a sum over all independent M channels.

Also, from selective excitation of the $M_f=M_g=J_f$ or $M_f=M_g-J_f$ channels with linear polarization we may separate two classes of molecules; those with the atom B (or A) precessing in the front of the polarization vector $\mathbf{e}_0$ and, vice versa, those with the atom A (or B) in front selected from the channel $M_f=M_g=J_f$ and $M_f=M_g-J_f$, respectively [17(c)]. Figure 1(b) shows that when Ω_f is not small compared to J_f (i.e., $\Omega_f/J_f=\frac{5}{9}$) the probability of exciting molecules with $\beta>\pi/2$ is very weak if the $M_f=M_g=J_f$ channel is excited. Inversely, through the $M_f=M_g=-J_f$ channel roughly only molecules with $\beta>\pi/2$ are excited. For a $^1\Sigma$ excited state, and in general for $\Omega_f/J_f\to 0$, both distributions coincide and are centered around the $\beta=\pi/2$ value. In Fig. 1(a) the shift of the two distributions associated with the channels $M_f=J_f$ and $-J_f$ stands for an intermediate case with $\Omega_f/J_f=\frac{1}{9}$.

In addition to the constrains for the orientation of the internuclear axis we have a further selection for the plane of molecular rotation. The importance of the orientation of the plane of molecular rotation in the excitation process is relevant in circular polarization. It is seen for instance that the channel $M_f=J_g+n$ (or $M_g=J_g$) is dominant in the $\Delta J=n$ rotational branch line; moreover, this dominance is further enhanced when the number of absorbed photons increases and thus a single orientation for the plane of rotation is favored for the above extreme rotational branch. This is shown in Fig. 1(c) for the NO $A\,^2\Sigma^+_{-1/2}\leftarrow X\,^2\Pi_{1/2}$ two-photon transition obtained from right circularly polarized radiation and for the $S(\frac{7}{2})$ branch line. We have the $M_f=M_g+n=-J_g+n,\ldots,J_g+n$ independent channels as potential

orientations for J_g with respect to the laser beam and we observe that the $M_g = J_g$ channel has the most favorably geometry for the excitation process if $p = 1$. For this particular channel the angular momentum is the most "well tied" around the laser beam (and thus around the CAM vector $\mathbf{n}$) and the orientation of the plane of molecular rotation remains unchanged. In contrast, for the remaining channels the transition from the $J_g M_g$ to the $J_f M_f$ state requires a change for the orientation of the plane of rotation; the higher the change the weaker the probability of exciting the corresponding channel. We observe in Fig. 1(d) that with increasing n the channels other than the channel $M_g = J_g$ (or $M_f = J_g + n$) become less probable and vanish rapidly.

The above observations show that excitation with circular polarization in the $|\Delta J| = n$ rotational branch favors only ground-state molecules with their angular momentum well tied along the laser beam while the angular momentum J_f in the excited state is also aligned along the laser beam. Nevertheless, for $\Delta J = n$, in general J_f is important compared to $|\Omega_f|$ and thus the internuclear axis is contained in a plane perpendicular to the laser beam rather than being aligned along this axis. This steric effect can be achieved, however, from the $\Delta J = -n$ rotational branch since in this case it is easy to obtain from selective excitation the condition $J_f = |\Omega_f|$ by decreasing the ground-state angular momentum quantum number by n units. In Fig. 1(e) we plot the case $\Omega_f / J_f = 1$ obtained

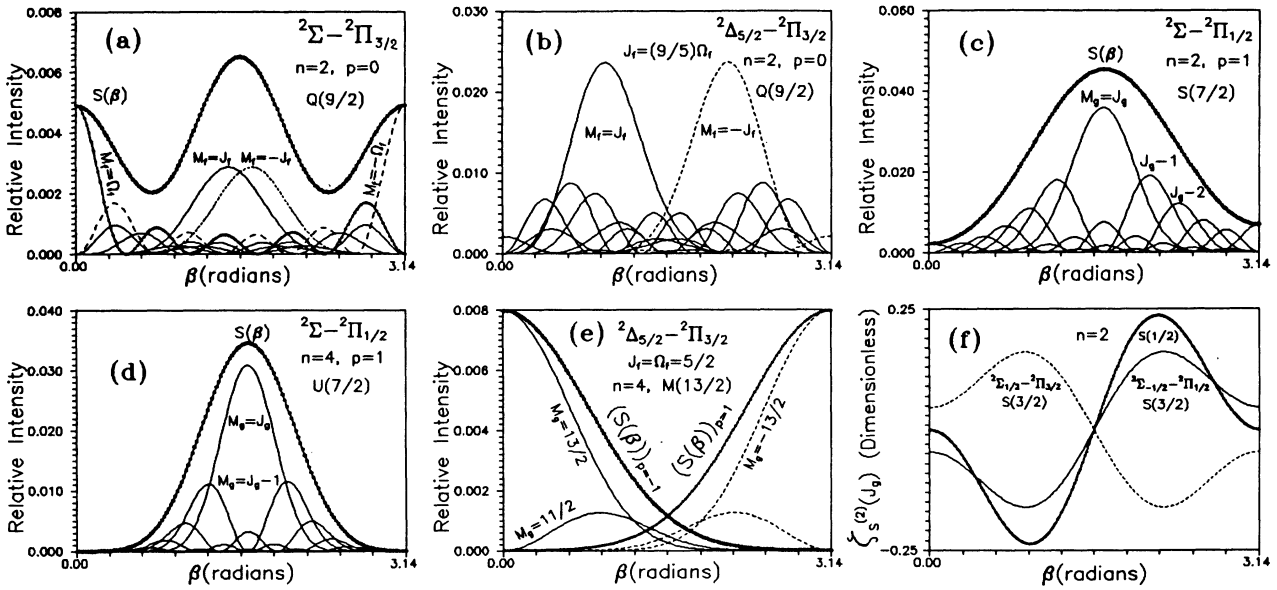

FIG. 1. (a) Selective excitation of the $M_f = \Omega_f$ sublevel with linear polarization leads to strong steric effects since this "resonant steric condition" favors only molecules with their internuclear axis collinear to the polarization vector [17(c)]. The $M_f = -\Omega_f$ resonant steric condition will select molecules with their axis anticollinear to the polarization vector. (b) From M-selective excitation of the $M_f = J_f$ or $-J_f$ sublevel with linear polarization we may separate two classes of molecules if $|\Omega_f|$ is not small compared to J_f. For instance, excitation of the $M_f = J_f$ sublevel in the above system selects A-B molecules with the atom B precessing in the front of the polarization vector [17(c)] and this precession is more "well tied" about the polarization vector as Ω_f approaches J_f. Instead, for a $^1\Sigma$ excited state, and in general for $|\Omega_f| \ll J_f$, the two distributions coincide and are centered around the $\beta = \pi/2$ value. (c) Excitation in the $\Delta J = n$ rotational branch with circular polarization selects molecules with their angular momentum well tied along the laser beam. Since for $p = 1$ or -1 the CAM vector is respectively collinear or anticollinear to the laser beam and $J_f = J_g + n$, the excitation process derives excited molecules with their angular momentum collinear or anticollinear to the laser beam. Here above, for $p = 1$, the $2J_g + 1$ channels $M_f = M_g + n = -J_g + n, \ldots, J_g + n$ only the channel $M_f = J_g + n$ (or $M_g = J_g$) has a favorable geometry for the excitation process. Thus even from M-unresolved excitation the selection of the plane of molecular rotation for the excited molecules is significant. (d) The effect described in (c) is considerably enhanced with increasing n. We observe that, for $p = 1$ and $\Delta J = n = 4$, the channels other than $M_g = J_g$ vanish rapidly. (e) Only one of the two atoms of the A-B molecule may be selected to point in the front of the laser beam. For instance, for the $\Delta J = -n$ rotational branch and excitation with left circularly polarized radiation ($p = -1$) only molecules with J_g oriented in the laser beam direction are favorably oriented. By decreasing the value of J_g by n units and thus obtaining $J_f = \Omega_f$ the angular momentum J_f is also oriented in the laser beam direction. The distribution of the internuclear axis is then centered around the laser beam direction. (f) The angular distribution of the internuclear axis in the excited state is prepared differently whether left or right circularly polarized radiation is involved. The photoionization signal obtained from the "prepared state" probes the dissimilarity and this can be measured by the DSE function $\zeta^{(n)}_{\Delta J}(J_g)$ given in Eq. (25). We observe that the two spin multiplets $\Omega_f = \frac{1}{2}$ and $-\frac{1}{2}$ of the NO $A\,^2\Sigma^+ \leftarrow X\,^2\Pi$ system have opposite dispersion functions.

from the $M(\frac{13}{2})$ rotational line with $\Delta J=-n=-4$ and for the $^2\Delta_{5/2}\leftarrow{}^2\Pi_{3/2}$ system. One remarks that for $p=-1$ only the $M_g=J_g$ ground-state J orientation is favored and this leads to strong steric effects even when the Zeeman structure is unresolved; this has been shown by the angular distribution of $S(\beta)$. Instead, for $p=1$ only the $M_g=-J_g$ channel is important and thus following excitation with left or right circularly polarized light the Ω_f vector [17(c)] is collinear or anticollinear to the laser beam. The above steric effect will be further enhanced with increasing Ω_f if the condition $J_f=\Omega_f$ is fulfilled.

Thus, even for M-unresolved levels, from multiphoton excitation with right and left circularly polarized light two classes of molecules can be prepared. This effect concerns heteronuclear diatomic molecules where only one of the two atoms of the molecule is present in the front of the laser beam; the distinction being more well specified when J_f approaches $|\Omega_f|$ since in this case the shift between the two distributions (associated with the two polarizations) approaches the π value. Instead, it can be seen that in the high-J limit (or for $\Omega_f/J_f=0$) the above shift vanishes and only molecules having their internuclear axis in a plane perpendicular to the laser beam are favorably oriented for the $|\Delta J|=n$ rotational branch. It is worth noting that in the plane perpendicular to the polarization vector the two distributions are always equal by symmetry.

The above "dichroic steric effect" (DSE) may be described by the DSE function

$$\zeta^{(n)}_{\Delta J}(J_g)=\frac{[S(\beta)]_{p=1}-[S(\beta)]_{p=-1}}{[S(\pi/2)]_{p=1}+[S(\pi/2)]_{p=-1}}\ , \tag{25}$$

which gives information on the penetration of one of the two atoms in the front of the laser beam. The DSE-function has been plotted in Fig. 1(f) for the NO $A\,^2\Sigma^+\leftarrow X\,^2\Pi_{1/2}$ two-photon transition and the $S(\frac{1}{2})$ branch line ($N_f=3, J_f=\frac{5}{2}$); this function involves an oriented excited state which is prepared differently from left or right circularly polarized radiation. We observe in the same graph that the two spin multiplets $^2\Sigma^+\leftarrow X\,^2\Pi_{1/2}$ and $^2\Sigma^+\leftarrow X\,^2\Pi_{3/2}$, for which $\Omega_f=-\frac{1}{2}$ and $\frac{1}{2}$ respectively, present opposite DSE functions. Furthermore, we remark a drastic dependence on J_g. In a pump-probe resonantly enhanced multiphoton ionization process of the NO $A\,^2\Sigma^+$ state via the $S_{21}(\frac{1}{2})$ rotational branch a very similar dependence with the DSE function is observed from the photoelectron angular distribution [18]. In this process, two-photon excitation with linear polarization is used to prepare the NO $A\,^2\Sigma^+$ state [instead of right and left two-photon excitation used for Fig. 1(f)] while one-photon ionization from this state with circular polarization probes the alignment. Then the above function is obtained by taking the difference between the photoionization signal with right and left circularly polarized incident radiation relative to the orientation where the photoionization signal is common for both polarizations.

IV. THE STERIC PARAMETER OF THE ANGULAR DISTRIBUTION

It seems clear that selective excitation of the $M_f=M_g=\Omega_f$ channel requires that the angular momentum J_f in the excited state presents a common projection both on the LFF and MFF quantization axes. This is a kind of a resonant steric condition and can be easily interpreted from the density probability of the internuclear axis orientation in the excited rotational state; this probability is proportional to $|d^{(J)}_{M\Omega}(\beta)|^2$ and it may be seen that for $M=\Omega$ we have $J-M+1$ potential orientations for the internuclear axis when β varies from 0 to π. However, the amplitude associated with the $\beta=0$ value is particularly enhanced compared to any other orientation. It follows that the most probable orientation satisfying the condition $M=\Omega$ is that with the internuclear axis pointing in the polarization vector direction. Inversely, the condition $M=-\Omega$ will enhance the orientation opposed to the polarization vector.

Thus, since the $M_f=M_g=\pm\Omega_f$ channels demand the above orientation for the internuclear axis, a significant alignment along the polarization vector should manifest in the excited state if only the $M_f=M_g=\pm\Omega_f$ channels were allowed to take place. This can be achieved by exciting the lowest rotational level of the ground state with linear polarization; i.e., the selection rules $M_f=M_g$ and $|M_g|\le J_g$ will permit only the channels $|M_f|\le J_g$ and thus for $J_g=\frac{1}{2}$ only the channels $M_f=M_g=\frac{1}{2}$ and $-\frac{1}{2}$ are present. In Fig. 2(a) we show the angular distribution for the $S(\frac{1}{2})$ branch line in the $A\,^2\Sigma^+(b)\leftarrow X\,^2\Pi_{1/2}(a)$ two-photon transition of the NO molecule. We observe that the alignment along the polarization vector is significant. We observe also a somehow weak probability of exciting molecules whose internuclear axis is found in a plane perpendicular to the polarization vector. This enables one to define a degree of alignment along the polarization vector and relatively to the plane perpendicular to this vector. For a given branch we introduce the steric parameter $\alpha^{(n)}_{\Delta J}$,

$$\alpha^{(n)}_{\Delta J}(J)=\frac{S(\beta=0)-S(\beta=\pi/2)}{S(\beta=0)+S(\beta=\pi/2)}\ , \tag{26a}$$

where ΔJ stands for the rotational branch and n for the number of photons absorbed. J will stand either for J_g or J_f. For the branch line considered in Fig. 2(a) we then obtain $\alpha^{(2)}_2(J_g=\frac{1}{2})=0.6$. It is important to remark that alignment along the polarization vector occurs only for rotational branches satisfying the condition $\Delta J+n=$even. Furthermore, the sharpest alignment is found to take place for the extreme rotational branch $\Delta J=n$. In Fig. 2(b) we show the angular distribution for the same system but obtained from six-photon excitation in the $\Delta J=6$ branch (W branch). The alignment parameter is considerably improved since we obtain $\alpha^{(6)}_6(J_g=\frac{1}{2})=0.83$.

In general, the alignment concerns unresolved M levels and this emerges whenever $J_g\ge|\Omega_f|$ and $\Delta J=n$, since in this case the $M_f=M_g=\pm\Omega_f$ channels are allowed to take place and, moreover, J_f is aligned along the laser

beam. Then, since excitation with linear polarization in the $\Delta J=n$ branch favors the $M_f=M_g=\pm\Omega_f$ channels and this exhibits an alignment for the internuclear axis along the polarization vector, it follows that if J_f is important compared to $|\Omega_f|$ (i.e., when n is important), the favorable geometry in space for the molecular system in the excitation process involves a plane of rotation perpendicular to the laser beam and, moreover, the internuclear axis must be aligned along the polarization vector. Thus the condition $\Delta J=n$ selects the plane of molecular rotation whereas the presence of the channels $M_f=M_g=\pm\Omega_f$ therein further selects aligned internuclear axes from this plane.

With the alignment parameter defined above and the sharpness of the distribution around the polarization vector being closely related we may introduce the enhancement quality factor (EQF) by the expression $\delta_{\Delta J}^{(n)}(J)=1/[1-\alpha_{\Delta J}^{(n)}(J)]$. We then obtain $\delta_2^{(2)}(J_g=\frac{1}{2})=2.5$, $\delta_4^{(4)}(J_g=\frac{1}{2})=4.1$, and $\delta_6^{(6)}(J_g=\frac{1}{2})=6$ for $\Delta J=2$, 4, and 6, respectively.

For rotational levels $J_g>\frac{1}{2}$ (or $J_g>1$) the degree of alignment and the corresponding EQF's decrease slowly since new channels are allowed. However, for the $\Delta J=n$ branch, these channels are significantly weak compared to the $M_f=M_g=\pm\Omega_f$ channels and thus a certain degree of alignment persists even for important values of J_g. This is shown in Fig. 2(c) for $J_g=\frac{9}{2}$, where we measure an alignment parameter $\alpha_2^{(2)}(J_g=\frac{9}{2})=0.52$ and an enhancement quality factor of 2.08 instead of 0.6 and 2.5 for $J_g=\frac{1}{2}$. Finally, we must note that there are particular branch lines for which the angular distribution of the internuclear axis is entirely isotropic. This is shown in Fig. 2(d) for the $Q(\frac{3}{2})$ branch line of the $^2\Sigma^+(b)\leftarrow{}^2\Pi_{3/2}(a)$ two-photon transition. Equally well, for $n=4,6,\ldots$ the angular distribution remains entirely isotropic.

The degree of alignment measured here is understood as alignment along the polarization vector of linearly polarized incident radiation. It is relevant to consider the

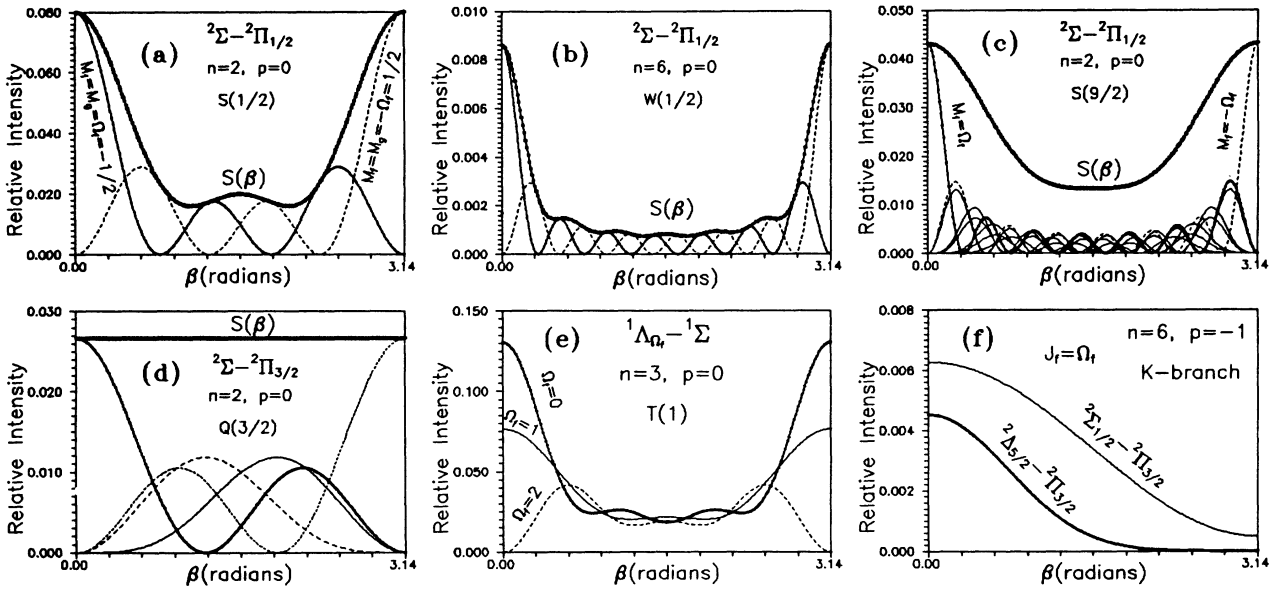

FIG. 2. In linear polarization, the selection rules $M_f=M_g$ and $|M_g|\leq J_g$ permit only the two channels $M_f=M_g=\frac{1}{2}$ and $-\frac{1}{2}$ if the lowest ground rotational level $J_g=\frac{1}{2}$ is selectively excited. Then, for an excited state with $|\Omega_f|=\frac{1}{2}$, an important alignment for the internuclear axis is present along the polarization vector. This alignment takes place only for rotational branches satisfying the condition $\Delta J+n=$even, and the sharpest alignment is found to take place for $\Delta J=n$. For the above system we obtain an alignment parameter $\alpha_2^{(2)}(\frac{1}{2})=0.6$ and an enhancement quality factor $\delta_2^{(2)}(\frac{1}{2})=2.5$. (b) The effect described in (a) is further enhanced with increasing n. For $n=6$ we obtain $\alpha_6^{(6)}(\frac{1}{2})=0.83$ and $\delta_6^{(6)}(\frac{1}{2})=6$. (c) For rotational levels with $J_g>\frac{1}{2}$ the degree of alignment and the corresponding enhancement quality factors decrease slowly since new channels are allowed. However, for the $\Delta J=n$ branch these channels are significantly weak compared to the $M_f=M_g=\pm\Omega_f$ channels and thus a certain degree of alignment persists even for high values of J_g. (d) For unresolved M levels we may have particular branch lines for which the angular distribution of the internuclear axis in the excited state remains entirely isotropic. For instance, for the above system, for $n=2,4,6,\ldots$ the angular distribution is equally well isotropic. (e) If alignment along the polarization vector is present this is due exclusively to the $M_f=M_g=\pm\Omega_f$ channels. This is shown by the dramatic decrease in the alignment when these specific channels are not allowed to take place, i.e., for $J_g=1$ the channels $M_f=\Omega_f=\pm2$ are absent for the $^1\Delta_2$ excited electronic state; then the probability of exciting a molecule with its internuclear axis aligned along the polarization vector vanishes. (f) The resonant steric condition $J_f=\Omega_f$ obtained from the $\Delta J=-n$ rotational branch with left circularly polarized light derives internuclear axis orientation in the laser beam direction. The degree of orientation is improved considerably when Ω_f increases. Here $[\alpha_K^{(6)}(\frac{13}{12})]_{\Omega_f=1/2}=0.3$ and $[\alpha_K^{(6)}(\frac{17}{2})]_{\Omega_f=5/2}=0.82$ for a $^2\Sigma_{1/2}$ and a $^2\Delta_{5/2}$ excited state, respectively.

absence of the $M_f=M_g=\pm\Omega_f$ channels; this leads to $\alpha_{\Delta J}^{(n)}(J)=-1$, which describes a forbidden orientation for the internuclear axis along the polarization vector, whereas, in contrast, if alignment is present the corresponding parameter has the unity as an asymptote. In Fig. 2(e) we show how drastically the alignment is modified when the channels $M_f=M_g=\pm\Omega_f$ are absent; this is plotted for the branch line $T(1)$ of the $^1\Lambda\leftarrow{}^1\Sigma$ three-photon transition with $\Lambda=0$, 1, and 2 (that is, for excited states $^1\Sigma_0$, $^1\Pi_1$, and $^1\Delta_2$). For the state $^1\Delta_2$ we have $\Omega_f=2$ whereas from the condition $|M_f|\le J_g$ it follows that the $M_f=M_g=\pm\Omega_f$ channels cannot take place if $J_g=1$. We then observe that the excited molecules cannot occupy at all any of the two orientations defined from the polarization vector.

Into this extension it is easy to define a steric parameter for the M channel. Similarly with the degree of alignment we define the expression

$$\alpha_{\Delta J}^{(n)}(J;M)=\frac{S(M;\beta=0)-S(M;\beta=\pi/2)}{S(\beta=0)+S(\beta=\pi/2)}\ , \tag{26b}$$

which describes the degree of orientation obtained from the M channel. If one sums over all M channels one will obtain $\alpha_{\Delta J}^{(n)}(J)$. It is understood that for the M channel also orientation is present and thus $S(M;0)\neq S(M;\pi)$. From Figs. 2(a), 2(b), and 2(c) we find, respectively, $\alpha_2^{(2)}(J_g=\frac{1}{2};\pm\frac{1}{2})=0.66$, $\alpha_6^{(6)}(J_g=\frac{1}{2};\pm\frac{1}{2})=0.86$, and $\alpha_2^{(2)}(J_g=\frac{9}{2};\pm\frac{1}{2})=0.72$. These values are somehow improved compared to the corresponding alignment and, moreover, they concern a single orientation in space.

In circular polarization, the degree of orientation for the internuclear axis around the polarization vector can also be measured from Eqs. (26a) and (26b). However, now the resonant steric condition for orientation of the internuclear axis along the polarization vector is given by $J_f=|\Omega_f|$ (instead of $M_f=\pm\Omega_f$ in linear polarization). This is obtained from the $\Delta J=-n$ rotational branch where we observe the sharpest distribution for large n and Ω_f. In Fig. 2(f) we plot $S(\beta)$ with the constraints, $J_f=\Omega_f$ and $\Delta J=-n$ for a six-photon process and $\Omega_f=\frac{1}{2}$ or $\frac{5}{2}$. The difference in the degree of orientation is considerable; from Eq. (26a) we obtain $[\alpha_K^{(6)}(J_g=\frac{13}{2})]_{\Omega_f=1/2}=0.3$ and $[\alpha_K^{(6)}(J_g=\frac{17}{2})]_{\Omega_f=5/2}=0.82$ for $\Omega_f=\frac{1}{2}$ and $\frac{5}{2}$, respectively.

V. ANGULAR DISTRIBUTION FOR UNRESOLVED-M LEVELS AND ROTATIONAL LINE STRENGTHS

When the Zeeman structure is unresolved one must sum over all degenerate M values. From Eq. (23) we obtain

$$S(\beta)=S_0\left\{1+\sum_{L=1}^{2n}\bar{\sigma}_{LO}P_L(\cos\beta)\right\}, \tag{27a}$$

where $\bar{\sigma}_{LO}=\bar{\sigma}_L/\bar{\sigma}_0$ and $S_0=\bar{\sigma}_0/(2J_g+1)$. The MOA tensor is given by

$$\bar{\sigma}_L=(2J_f+1)\sum_k(2k+1)\bar{c}_{kk}^{(n)}(p)\begin{pmatrix}k&0&k\\-np&0&np\end{pmatrix}\times\begin{pmatrix}k&L&k\\-np&0&np\end{pmatrix}\begin{Bmatrix}k&k&L\\J_f&0&J_f\\J_g&k&J_f\end{Bmatrix}\Theta_{kk}^{(L)}\mathcal{C}\ . \tag{27b}$$

As previously, the sum over k obeys to $k=n,n-2,\ldots,|\Delta\Lambda|$.

Now we observe that the number of Legendre polynomials involved in the angular distribution of the internuclear axis is determined exclusively from the number of photons absorbed and no longer from the excited rotational level. Moreover, in linear polarization only the even values of L are allowed. Since $P_L(1)=1$ and $P_L(-1)=(-1)^L$ we obtain $S(0)=S(\pi)$ and thus only alignment for the internuclear axis may be present in this case.

The tensor S_0, which constitutes the amplitude of the distribution, is the isotropic rotational line strength of the process. For any CCS we obtain

$$S_0=\frac{1}{2J_g+1}\sum_k\frac{1}{2k+1}\bar{c}_{kk}^{(n)}(p)\Theta_{kk}^{(0)}\mathcal{C}\ . \tag{28}$$

In the CCS b-b the rotational line factor is given by

$$\Theta_{kk}^{(0)}(\text{b-b})=(2J_g+1)(2N_g+1)(2J_f+1)(2N_f+1)\times\begin{pmatrix}N_g&k&N_f\\\Lambda_g&\Delta\Lambda&-\Lambda_f\end{pmatrix}^2\begin{Bmatrix}N_f&k&N_g\\J_g&S&J_f\end{Bmatrix}^2\ . \tag{29}$$

If we set $S=0$ and replace Λ by Ω and N by J we obtain the case sequence a-a rotational line strength. Singlet transitions are particular cases, obtained by setting $S=0$ in Eq. (29).

From the coefficient $\bar{c}_{kk}^{(n)}(0)/(2k+1)$ and from Table II of Appendix A we observe that, in linear polarization, the k term is always weaker than the $(k-2)$ term. Furthermore, the xj symbols involved therein may further decrease the terms corresponding to high-k values. It follows that the higher the values for the CAM quantum numbers, the lower their probability of occurrence since these values are associated with a high number of MFF dipole components having the same orientation. Since transitions involving a large change in the rotational quantum number are associated with high CAM quantum numbers, it follows that the extreme rotational branches in a n-photon process decrease gradually.

The angular distribution for unresolved M levels, given in Eq. (27), can be explicitly determined both for linear and circular polarization. Therefore an analytic expression for the steric parameter $\alpha_{\Delta J}^{(n)}(J)$, which has been defined by Eq. (26a), may be obtained. Given that $P_L(0)=0$ if L is odd and $(-1)^{L/2}(L-1)!!/L!!$ if L is

even we find

$$\alpha_{\Delta J}^{(n)}(J)=\frac{S(\beta=0)-S(\beta=\pi/2)}{S(\beta=0)+S(\beta=\pi/2)}=\left[\sum_{L=1}^{2n} d_L^{-}\bar{\sigma}_L\right]\Big/\left[2\bar{\sigma}_0+\sum_{L=1}^{2n} d_L^{+}\bar{\sigma}_L\right], \quad (30)$$

with $d_L^{\pm}=1\pm\delta_{L,\text{even}}(-1)^{L/2}[(L-1)!!/L!!]$ and $\delta_{L,L'}$ the Kronecker symbol.

In circular polarization, both the even and odd values of L are allowed to take place in the $\bar{\sigma}_L$ tensor. Therefore, $S(0)\neq S(\pi)$ in this case and the steric parameter measures orientation relatively to the plane perpendicular to the laser beam.

For unresolved M levels the amplitude of the angular distribution is given by rotational line strength S_0. Therefore, $S(\beta)$ gives also information on the intensity distribution among the rotational branches. Furthermore, the isotropic rotational line strength S_0 may be written both for linear and circular polarization and thus furnish information on the polarization intensity ratio of a given rotational branch. For instance, in the particular case of the four extreme rotational branches where only the $k=n$ value is allowed we obtain $(S_0^{\text{lin}})/(S_0^{\text{cir}})=\bar{c}_{nn}^{(n)}(0)=1, \frac{2}{3}, \frac{2}{5}, \frac{8}{35}, \ldots$ for $n=1,2,3,4,\ldots$, respectively.

In Fig. 3(a) we plot $S(\beta)$ from Eq. (27) for a three-photon excitation in the $^1\Pi\leftarrow{}^1\Sigma$ system. The angular distribution of the different rotational branches is shown for the excited levels obtained from the $J_g=5$ ground rotational level. We observe that the N, O, S, and T branches present only a weak excitation probability whereas the Q and R branches are enhanced. The above intensity distribution agrees with the observed three-photon excitation spectra of the CO $A\,^1\Pi\leftarrow X\,^1\Sigma^+$ system which show enhanced Q and R branches and a P branch with a somewhat reduced intensity. The authors report that the N, O, S, and T branches are too weak to be observed [19]. The intensity distribution among the rotational branches in a n-photon electronic transition can also be observed from conventional photoelectron spectra obtained from the excited state. For a given intermediate excited level J_f the intensity of the photoionization signal will depend on the involved rotational branch line $\Delta J=J_f-J_g$. In

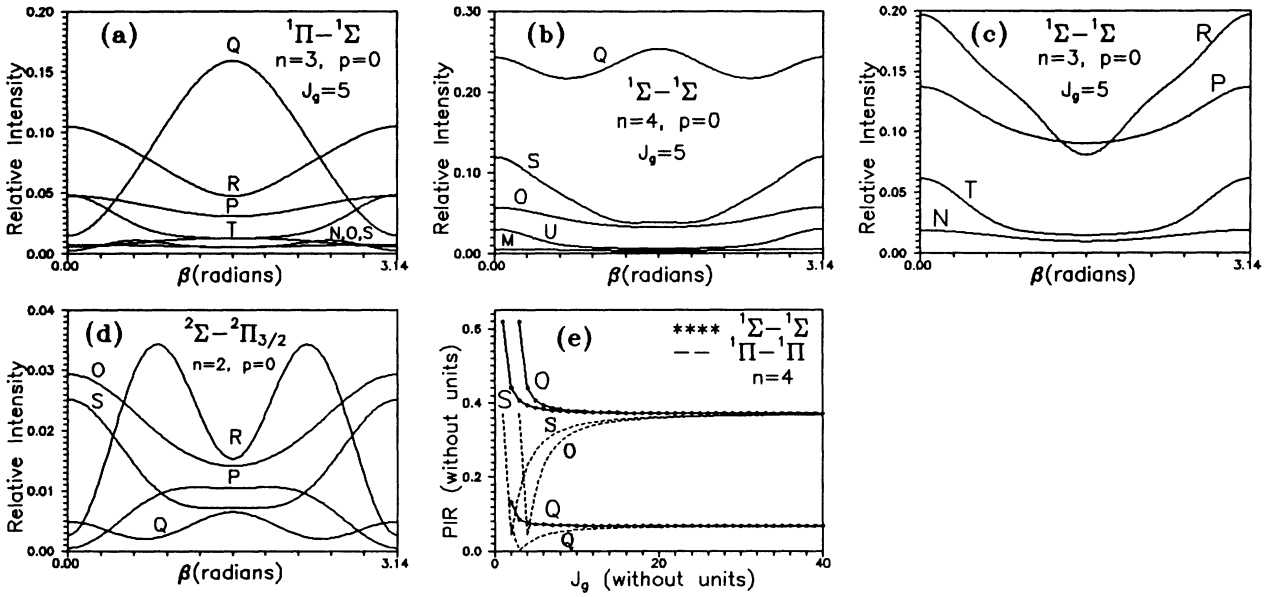

FIG. 3. (a) The angular distribution of the internuclear axis gives also information on the intensity distribution among the rotational branches. Here, in three-photon excitation in the CO $A\,^1\Pi\leftarrow X\,^1\Sigma^+$ system, the N, O, S, and T branches present only weak intensities whereas the Q and R branches are enhanced. Each rotational branch presents a distinct angular distribution. (b) In a four-photon transition in the $^1\Sigma\leftarrow{}^1\Sigma$ system the Q branch is particularly enhanced and is followed by weaker S and O branches. The extreme M and U branches appear particularly weak as expected. (c) The three-photon excitation spectra in the $^1\Sigma\leftarrow{}^1\Sigma$ system show strong P and R branches followed by the N and T branches with only weak intensities. For the $\Delta J=\pm1,\pm3$ branches ($\Delta J+n$ even) one observes that, although the angular distribution is roughly the same when it is observed in the plane perpendicular to the polarization vector, along this vector, the anisotropy between positive and negative ΔJ branches is relevant. (d) For the two-photon excitation of the NO $A\,^2\Sigma^+\leftarrow X\,^2\Pi_{3/2}$ system through the $\Delta J=2$ rotational branch (S branch) the angular distribution of the internuclear axis in the excited state shows an alignment along the polarization vector. Further photoionization of this state probes the alignment by the observed photoelectron angular distribution [24]. Also, the anisotropic distribution of the internuclear axis in the excited state leads to an anisotropic fluorescence signal when this is detected at $\beta=0$ or at $\beta=\pi/2$. (e) The polarization intensity ratio for the four extreme rotational branches is given by $S^{\text{cir}}/S^{\text{lin}}=1/\bar{c}_{nn}^{(n)}(0)=1,\frac{3}{2},\frac{5}{2},\frac{35}{8},\ldots$ for $n=1,2,3,4,\ldots$, respectively; this simple expression arises since only the extreme CAM value is allowed to take place. However, for the remaining branches, only for high-J values the intensity ratio approaches a constant value whereas this constant depends on the rotational branch involved. For low rotational levels we observe a drastic dependence, both in the rotational branch as well as in the symmetry of the electronic states.

fact, photoelectron studies of resonant multiphoton ionization for the CO molecule via the $A\,^1\Pi$ state [20] confirm the absence of the N, O, S, and T branches, the recorded CO^+ signal shows only the P, Q, and R branches. Similarly, photoionization of the excited H_2 $C\,^1\Pi_u$ state, prepared by three-photon excitation, shows lack of the N, O, S, and T branches [21].

The band structure of the photoelectron spectra in the vibrational band of the $N_2^+\ X\,^2\Sigma_g^+ \leftarrow N_2 X\,^1\Sigma_g^+$ and for transitions with $\Delta J = 0, \pm 2, \pm 4$ has been already observed; the ionizing radiation is produced by a microwave powered electron-cyclotron-resonance source and the spectra show an enhanced Q branch followed by weaker S and O branches [22,23]. Furthermore, the S branch appears more intense than the O branch whereas the M and U branches are particularly weak to be observed. The above observations are similar with those obtained from the four-photon $^1\Sigma \leftarrow {}^1\Sigma$ transition which is shown in Fig. 3(b). On the other hand, the three-photon excitation spectra in the $^1\Sigma$-$^1\Sigma$ system show strong P and R branches (with the P branch more intense for $\beta = \pi/2$ than at $\beta = 0$) following by the N and T branches with only weak intensities. This is shown in Fig. 3(c), which is very close to the observed intensity distribution of the $\Delta J = \pm 1, \pm 3$ branches in the $N_2^+ B\,^2\Sigma_u^+ \leftarrow N_2 X\,^1\Sigma_g^+$ photoelectron spectra [22]. Thus the above observed intensities are essentially determined from the symmetry of the electronic states and the involved rotational branch.

The rotational branches with $\Delta J + n = \text{even}$ present an alignment around the polarization vector and when ΔJ is positive the corresponding alignment is more important than the alignment of the $-\Delta J$ branch line. Thus the intensities may differ significantly if they are observed along the polarization vector in a plane perpendicular to this vector; for example, in Fig. 3(b) the $S(5)$ branch line is two times more intense than the $O(5)$ branch line if this intensity is observed along the polarization vector whereas both of them have equivalent intensities in the plane perpendicular to the polarization vector. Similar observations can be made for the U and M branches as well as for the P, R, N, and T branch lines of Fig. 3(c). This leads to anisotropic rotational line profiles in the photoelectron energy spectra when positive and negative ΔJ branches are involved. In general, this anisotropy is different for intensities observed along the polarization vector of linearly polarized radiation or in a plane perpendicular to this vector.

In Fig. 3(d) we plot $S(\beta)$ for the $N_f = 4, J_T = \frac{9}{2}$ rotational level and for the different rotational branches ΔJ which may take place in the NO $A\,^2\Sigma^+ \leftarrow X\,^2\Pi_{3/2}$ two-photon transition with linear polarization. The ionization step from the $A\,^2\Sigma^+$ excited state being predominantly parallel, the transition dipole is parallel to the internuclear axis. Photoelectron spectra resulting from the two-photon resonance four-photon ionization via the S branch of the NO $A\,^2\Sigma^+ \leftarrow X\,^2\Pi_{3/2}$ system [24(a)] show a photoelectron angular distribution for the two final ionic vibrational states $v = 0$ and 1 similar [24(b)] to the angular distribution of the internuclear axis in the intermediate excited state. This suggests that the internuclear axis in the intermediate excited state is aligned along the polarization vector when the extreme rotational branch is involved.

The anisotropic distribution of the internuclear axis in the excited state can also be probed from the fluorescence anisotropy detected at $\beta = 0$ and $\pi/2$. Measurement of the fluorescence anisotropy of the isolated $O_{12}(7.5)$ branch line from excited NO* $A\,^2\Sigma^+$ molecules produced by two-photon excitation shows a signal at $\beta = 0$ stronger than that at $\beta = \pi/2$ [25]. The observed anisotropy in these spectra, however, is weaker than the anisotropy depicted from the O branch of Fig. 3(d).

Similar studies for the intensity distribution in the rotational branches may be done for other multiphoton processes. For instance, if we draw the two-photon excitation probability of the $^1\Sigma \leftarrow {}^1\Sigma$ system as a function of the angle β we observe that the excitation probabilities for the S and O branches are low compared to that of the Q branch. It is also seen that circularly polarized light gives a Q branch with an intensity equivalent to that of the S and O branches. In fact the two-photon excitation spectra of the CO $B\,^1\Sigma^+ \leftarrow X\,^1\Sigma^+$ transition, obtained with linear polarization, show an intense Q branch which dominates the transition [26].

On the other hand, the two-photon excitation of the $^1\Pi \leftarrow {}^1\Sigma$ system obtained with linearly polarized light reveals a very weak Q branch. The most intense branch now is the S branch, which is at least 25 times more intense than the Q branch. The observed excited fluorescence in the two-photon excitation spectra of the CO fourth positive system [27,28] $A\,^1\Pi \leftarrow X\,^1\Sigma^+$ reveals an enhanced S branch and a Q branch of particularly weak intensity. Moreover, in the two-photon resonant, four-photon ionization of CO via the $A\,^1\Pi$ state, reported measurements of photoelectron spectra confirm this enhancement [29].

Similar observations can be made for the two-photon excitation of the metastable upper state of the Lyman-Birge-Hopfield system $a\,^1\Pi_g \leftarrow X\,^1\Sigma_g^+$ in N_2 [30]. Finally, we plot in Fig. 3(e) the polarization intensity ratio (PIR) $S_0^{\text{cir}}/S_0^{\text{lin}}$ for the O, Q, and S branches of a four-photon process. We observe that the ΔJ and $-\Delta J$ branches approach the same PIR value only with increasing J, whereas for low J, the anisotropy between these two opposite branches is relevant. Moreover, this anisotropy depends drastically on the electronic states when the J values are low. For the extreme rotational branches where only the $k = n$ value is allowed, however, the intensity ratio is always constant and equals $\frac{35}{8}$ for any J.

VI. IMPORTANT PARTICULAR CASES AND CONCLUDING REMARKS

When at least one of the two electronic states belongs to case (a) the spin angular momentum is "tied" to the internuclear axis and important simplifications occur. This arises since in electric dipole allowed transitions the spin component Σ is common for both states. Furthermore, for a given M channel, when the polarization of the incident radiation is linear the angular distribution becomes independent of the number of absorbed photons. In such circumstances only the amplitude of the distribu-

tion depends on the order of the nonlinear process and, more generally, how the specific state is populated.

In fact, when at least one of the two states belongs to case (a), from Eqs. (22) and (B5) it follows that the MOAP tensor of Eq. (23) simplifies to the expression

$$\bar{\sigma}_{LO}(M)=(2L+1)(2J_f+1)^2\begin{pmatrix} J_f & 0 & J_f \\ -M_f & 0 & M_f \end{pmatrix} \times \begin{pmatrix} J_f & L & J_f \\ -M_f & 0 & M_f \end{pmatrix}\begin{pmatrix} J_f & 0 & J_f \\ -\Omega_f & 0 & \Omega_f \end{pmatrix} \times \begin{pmatrix} J_f & L & J_f \\ -\Omega_f & 0 & \Omega_f \end{pmatrix}, \tag{31}$$

where $\Omega_f=\Lambda_f+\Sigma$ and $M_f=M_g+np$. We observe that now the MOAP tensor depends exclusively on J_f and its projections on the LFF and MFF quantization axes. Moreover, in linear polarization, $\bar{\sigma}_{LO}(M)$ becomes independent of n since for this case we have $M_f=M_g$.

Then it may be seen from Eq. (23) that the probability of exciting the state $|J_fM_f\Omega_f\rangle$ from the ground state $|J_gM_g\Omega_g\rangle$ when the internuclear axis of the molecule forms an angle β with the polarization vector of the incident radiation simplifies to

$$S(M_f;\beta)=(2J_f+1)S(M_f)[d^{(J_f)}_{M_f,\Omega_f}(\beta)]^2, \tag{32}$$

where $M_f=M_g+np$, $\Omega_f=\Lambda_g+\Sigma+\Delta\Lambda$, and $J_f=J_g+\Delta J$ with $\Delta J=0,\pm1,\ldots\pm n$; otherwise the excitation probability vanishes. In Eq. (32), $S(M_f)=\frac{1}{2}\int_0^\pi \sin\beta\, d\beta S(M_f;\beta)$ concerns the β-averaged probability of populating the sublevel $M_f=M_g+np$. We observe that also the ratio $S(M_f;\beta)/S(M_f)$ depends exclusively on J_f and its projections on the LFF and MFF quantization axes. The quantity $S(M_f)$ is the relative occupation probability of the M_f sublevel, which is given by

$$S(M_f)=s^{\mathrm{CCS}}(\Sigma)(2J_f+1) \times \sum_k \bar{c}^{(n)}_{kk}(p)\begin{pmatrix} J_g & k & J_f \\ M_g & np & -M_f \end{pmatrix}^2 \times \begin{pmatrix} J_g & k & J_f \\ \Lambda_g+\Sigma & \Delta\Lambda & -\Lambda_f-\Sigma \end{pmatrix}^2, \tag{33}$$

with $s^{\mathrm{CCS}}(\Sigma)$, the spin-multiplicity weighting factor. This is $s^{aa}(\Sigma)=1$ for the a-a case and

$$s^{ab}(\Sigma)=(2N_f+1)\begin{pmatrix} J_f & S & N_f \\ \Lambda_f+\Sigma & -\Sigma & -\Lambda_f \end{pmatrix}^2$$

or

$$s^{ba}(\Sigma)=(2N_g+1)\begin{pmatrix} J_g & S & N_g \\ \Lambda_g+\Sigma & -\Sigma & -\Lambda_g \end{pmatrix}^2 \tag{34}$$

for the case a-b or the b-a case transitions, respectively. Singlet transitions are particular cases; they are obtained by setting $S=\Sigma=0$ and replacing J by N everywhere.

The quantities $d^{(j)}_{m'm}(\beta)$ are the matrix elements of finite rotations which are always real [31,13] and their square conjugate defines the shape of the angular distribution. Note that $(2J_f+1)[d^{(J_f)}_{M_f\Omega_f}(\beta)]^2$ is the density probability of finding an angle β between the internuclear axis and the polarization vector in the final rotational state. Then by inspecting Eq. (32) we observe that $S(M_f;\beta)$ representing the required molecular angular distribution for the excitation process; this is simply given by the orientation density probability of the final rotational state multiplied by the probability strength of the $M_f=M_g+np$ channel and the spin-multiplicity weighting factor $s^{\mathrm{CCS}}(\Sigma)$. Thus, if the internuclear axis or the plane of molecular rotation are not favorably oriented for the excited rotational state, the excitation probability becomes weak. The most simple case considering how the plane of rotation has to be oriented in order to populate efficiently an excited state is the case of the $M_f=J_f$ sublevel in a $^1\Sigma$ excited electronic state. For this particular case the angular distribution becomes proportional to $(\sin\beta)^{2J_f}$ and thus, with increasing molecular rotation, the internuclear axis becomes increasingly well confined in the plane perpendicular to the polarization vector.

Since the angular distribution for the internuclear axis in the excitation process becomes proportional to the quantity $[d^{(J_f)}_{M_f\Omega_f}(\beta)]^2$, the properties $[d^{(J)}_{M\Omega}(0)]^2=\delta_{M,\Omega}$ and $[d^{(J)}_{M\Omega}(\pi)]^2=\delta_{M,-\Omega}$ lead to the following selection rules.

(i) When one is concerned with oriented molecules having their internuclear axis collinear to the polarization vector excitation of some rotational line populates predominantly the $M_f=\Omega_f$ corresponding sublevel.

(ii) On the other hand, M-selective excitation of the $M_f=\Omega_f$ (or $M_f=-\Omega_f$) sublevel from an initially isotropic distribution will result in an enhanced β anisotropy for the excited molecules, the angular momentum $\boldsymbol{\Omega}_f$ being oriented along the polarization vector with $\beta=0$ or π following the case $M_f=\Omega_f$ or $-\Omega_f$, respectively.

A similar expression as Eq. (32) can also describe the angular distribution of oriented molecules in the ground state. In fact, ground-state rotationally state-selected molecules in a molecular beam can be oriented by hexapole field techniques followed by a dipole orienting field [32]. These techniques can provide a relatively well-specified orientation. Nevertheless, this concerns ground-state molecules which are assumed to have a permanent electric dipole moment and, furthermore, are subject in strong electric fields.

In M-resolved experiments the magnetic sublevels reveal important steric properties and if one of the two electronic states belongs to Hund's case a these effects obey to simple expressions. For instance, from selective excitation of the particular $M_f=\Omega_f$ sublevel, by virtue of the β dependence of the excitation probability we create an oriented excited state for which the initial angular distribution is determined by $(2J_f+1)[d^{(J_f)}_{\Omega_f,\Omega_f}(\beta)]^2$. One then remarks that the excitation probability is enhanced only around the $\beta=0$ value and becomes sharper with increasing molecular rotation, whereas for $\beta=\pi$ it van-

ishes. Thus the internuclear axes of the excited molecules have the same initial orientation and they start to precess about their angular momenta while for times $T, 2T, \ldots$ they occupy repeatedly the same orientation in space.

It is clear that [apart from the fact that the population of the excited level is given by $S(M_f)$ and thus it depends on the order of the excitation process] in M-resolved experiments the degree of orientation is independent of how the oriented excited state has been prepared. For a given process the degree of orientation depends exclusively on the excited rotational state. However, if the magnetic levels are unresolved the ratio of oriented over unoriented molecules is formed from Eq. (27) and leads to $[S(\beta)/S_0]=\sum_{L=0}^{2n}\bar{\sigma}_{LO}P_L(\cos\beta)$, which for $\beta=0$ reduces to $(1+\sum_{L=1}^{2n}\bar{\sigma}_{LO})$. Thus the degree of orientation now depends explicitly on the excitation process and we have an isotropic excited state only if $\bar{\sigma}_L=0$ for all $L\geq 1$ [33]. This shows that, even for M-unresolved levels, the angular distribution of the internuclear axis in the excited state is anisotropic. The sharpest anisotropy for M-unresolved levels is found to take place for the extreme rotational branches $\Delta J=\pm n$ and it is enhanced with increasing n. In general, the angular distribution is described either by $S(M;\beta)$ or $S(\beta)$ following the case of resolved or unresolved magnetic levels and these expressions can be plotted for any nonlinear process; the β-averaged expression then describe the relative occupation probability of the corresponding rotational lines.

The degree of orientation for the internuclear axis obtained from the multiphoton process can be measured by the steric parameter introduced by Eq. (26). For the rotational subline $N_gJ_gM_g\rightarrow N_fJ_fM_f$ it results in

$$\alpha_{\Delta J}^{(n)}(J;M)=\left[\sum_{L=1}^{2J_f} d_L^{-}\bar{\sigma}_L(M)\right]\Big/\left[2\bar{\sigma}_0+\sum_{L=1}^{2n} d_L^{+}\bar{\sigma}_L\right], \tag{35}$$

while, for unresolved M levels a summation over all M levels is required and leads to the steric parameter $\alpha_{\Delta J}^{(n)}(J)$ of Eq. (30), which, for linear polarization, describes only alignment. For instance, by exciting the lowest ground rotational level of the NO $A\,^2\Sigma^+\leftarrow X\,^2\Pi_{1/2}$ system with linear polarization, from the extreme rotational branch $\Delta J=n$ we obtain an alignment with $\alpha_2^{(2)}(J_g=\frac{1}{2})=0.6$, $\alpha_4^{(4)}(J_g=\frac{1}{2})=0.75$, and $\alpha_6^{(6)}(J_g=\frac{1}{2})=0.83$ for $n=2$, 4, and 6, respectively. Besides, from $M_f=M_g=\Omega_f$ or $=-\Omega_f$ selective excitation the corresponding steric parameter is somehow improved and, moreover, it describes a single orientation in space. Finally, it is worth noting that, although for unresolved-M levels and the $\Delta J=n$ rotational branch the sharpness of the alignment decreases with increasing J_g [34], in contrast, from M-selective excitation the sharpness of the angular distribution is further improved with increasing J_g.

Thus the $M_f=M_g=\pm\Omega_f$ channels in linear polarization and the $J_f=|\Omega_f|$ condition in circular polarization together with the $\Delta J=\pm n$ rotational branches contain important steric effects; in addition, these effects are considerably enhanced by multiphoton excitation. Molecular excited states prepared under the above resonant steric conditions are expected to show strong steric effects in their fluorescence, their photoelectron angular distribution, or in the chemiluminescence of their chemical reactions.

ACKNOWLEDGMENT

The author is grateful to Professor J. Baudon for a critical reading and helpful suggestions.

APPENDIX A

In this appendix we show that the tensor

$$\bar{c}_{kk'}^{(n)}(p)=\beta_{k,np}\beta_{k',np}\sum_{\alpha}\mathcal{A}(\alpha)B_k^{(n)}(\alpha)B_{k'}^{(n)}(\alpha) \tag{A1}$$

vanishes whenever $k'\neq k$ and we calculate the diagonal terms of this tensor for up to seven-photon processes. In fact the β and B tensors emerge from the contraction of the n rotation matrix elements $\mathcal{D}_{p,q}^{(1)*}(\alpha\beta\gamma)$, which transform the electric dipole operator from the LFF into the MFF for every absorbed photon. They may be contracted by considering the first two elements and then contracting the obtained result with the third one. By successive operations we obtain [11]

$$\mathcal{D}_{p,q_n}^{(1)*}\cdots\mathcal{D}_{p,q_1}^{(1)*}=\sum_k\beta_{k,np}B_k^{(n)}(q_1\cdots q_n)_{Q_n}\mathcal{D}_{-np,-Q_n}^{(k)}, \tag{A2}$$

TABLE I. The tensor $B_k^{(4)}(\alpha)_{Q_4}$.

Q_4	α	$\mathcal{A}(\alpha)$	0	2	4
0	(0000)	1	$-\sqrt{9/75}$	$+\sqrt{144/1470}$	$-\sqrt{16/22\,050}$
	(001-1)	12	$+\sqrt{1/75}$	$-\sqrt{1/1470}$	$-\sqrt{4/22\,050}$
	(1-11-1)	6	$-\sqrt{4/75}$	$-\sqrt{16/1470}$	$-\sqrt{1/22\,050}$
1	(0001)	4	0	$-\sqrt{9/490}$	$+\sqrt{4/8820}$
	(01-11)	12	0	$+\sqrt{4/490}$	$+\sqrt{1/8820}$
2	(0011)	6	0	$+\sqrt{1/245}$	$-\sqrt{4/8820}$
	(1-111)	4	0	$-\sqrt{9/245}$	$-\sqrt{1/8820}$
3	(0111)	4	0	0	$+\sqrt{1/1260}$
4	(1111)	1	0	0	$-\sqrt{1/315}$

TABLE II. The tensor $\bar{c}_k^{(n)}(0)$.

$k \backslash n$	1	2	3	4	5	6	7	8
0	0	$\frac{1}{3}$	0	$\frac{1}{5}$	0	$\frac{1}{7}$	0	
1	1	0	$\frac{3}{5}$	0	$\frac{3}{7}$	0	$\frac{3}{9}$	
2		$\frac{2}{3}$	0	$\frac{4}{7}$	0	$\frac{10}{21}$	0	
3			$\frac{2}{5}$	0	$\frac{4}{9}$	0	$\frac{14}{33}$	
4				$\frac{8}{35}$	0	$\frac{24}{77}$	0	
5					$\frac{8}{63}$	0	$\frac{8}{39}$	
6						$\frac{16}{231}$	0	
7							$\frac{16}{429}$	
8								

where $Q_n = q_1 + q_2 + \cdots + q_n$ and k is the composite angular momentum quantum number which takes the integer positive values with the conditions $O \leq k \leq n$ and $k+n$ even; otherwise the tensor $\beta_{k,np}$ will vanish. From previous work it follows [10,11] that the β tensor can be written as $\beta_{k,0} = (-1)^{\Phi}\delta_{k+n,\text{even}}\sqrt{(2k+1)k!/3}$ or $\beta_{k,\pm n} = (-1)^{\Phi}\delta_{k,n}\sqrt{(2n+1)!!/3}$ for linear or circular polarization, respectively. The phase factor is given by $\Phi = np + (k+2)/2$ if n is even and $\Phi = np + (k+3)/2$ if n is odd. We see that the sense of polarization has no effect on this tensor.

All the tensor components $B_k^{(n)}(q_1 \cdots q_n)_{Q_n}$ may be derived from a recursion formula [10] and from the lowest rank tensor $B_1^{(1)}(q)_q = (-1)^{-q}$. The above tensor is nonvanishing only when $n \geq k \geq |Q_n|$. Below we derive the tensor $B_k^{(4)}(\alpha)_{Q_4}$ for its allowed transition paths.

It may be easily verified from Table I that, since the tensor $\bar{c}_{kk'}^{(n)}(p)$ involves an averaging over all transition paths α with $\mathcal{A}(\alpha)$ as transition path weighting factor, only diagonal terms for k are nonvanishing. For instance, we find that the quantity $\sum_\alpha \mathcal{A}(\alpha) B_k^{(4)}(\alpha)_{Q_4} B_{k'}^{(4)}(\alpha)_{Q_4}$ vanishes whenever $k' \neq k$. This is more general and holds for any n and Q_n. Furthermore, it may be verified that any diagonal term for the above quantity brings the same unique value independently of the particular value of Q_n.

It follows that the tensor $\bar{c}_{kk}^{(n)}(p)$ is independent from Q_n and depends exclusively on n and k. The symmetries of the initial and final electronic states only contribute through the number of allowed CAM vectors which obey the selection rule $|\Delta\Lambda| \leq k \leq n$.

For circular polarization only the $k=n$ value is allowed. Then we find $\bar{c}_{nn}^{(n)}(1) = \bar{c}_{nn}^{(n)}(-1) = 1$. For linear polarization the tensor $\bar{c}_{kk}^{(n)}(0) = \frac{1}{3}(2k+1)k!\sum_\alpha \mathcal{A}(\alpha)|B_k^{(n)}(\alpha)_{Q_n}|^2$ is derived in Table II for up to seven-photon processes. We remark that the extreme values $\bar{c}_{nn}^{(n)}(0)$ give the polarization intensity ratio of the four extreme rotational branches $|\Delta J| = n$ and $n-1$ for any electronic transition.

APPENDIX B

In Eq. (14), the RLA tensor holds for the b-b coupling case sequence where both the ground and excited states belong to Hund's case (b) coupling. However, for the particular case of singlet molecular states ($S=0$) there is no way to distinguish case (a) and case (b) coupling. In this case the molecular states may be treated equally well by either coupling scheme. Setting $S=0$ in Eq. (14) and replacing Λ by Ω everywhere we obtain

$$\Theta_{kk'}^{(L)}(\text{a-a}) = (2L+1)(2J_g+1)(2J_f+1)^2 \times \begin{bmatrix} J_f & 0 & J_f \\ -\Omega_f & 0 & \Omega_f \end{bmatrix} \begin{bmatrix} J_f & L & J_f \\ -\Omega_f & 0 & \Omega_f \end{bmatrix} \times \begin{bmatrix} J_g & k & J_f \\ \Omega_g & \Delta\Omega & -\Omega_f \end{bmatrix} \begin{bmatrix} J_g & k' & J_f \\ \Omega_g & \Delta\Omega & -\Omega_f \end{bmatrix}. \tag{B1}$$

This is the a-a case RLA tensor. To obtain Eq. (B1) we have used the identity

$$\sum_{N_g'} (2N_g'+1) \begin{bmatrix} N_g' & L & J_g \\ -\Omega_g & 0 & \Omega_g \end{bmatrix} \begin{bmatrix} J_f & k' & N_g' \\ \Omega_f & -\Delta\Omega & -\Omega_g \end{bmatrix} \begin{bmatrix} J_f & k' & N_g' \\ J_f & J_f & L \\ 0 & J_g & J_g \end{bmatrix} = \begin{bmatrix} J_g & 0 & J_g \\ -\Omega_g & 0 & \Omega_g \end{bmatrix} \begin{bmatrix} J_f & 0 & J_f \\ -\Omega_f & 0 & \Omega_f \end{bmatrix} \begin{bmatrix} J_f & L & J_f \\ -\Omega_f & 0 & \Omega_f \end{bmatrix} \begin{bmatrix} J_f & k' & J_g \\ -\Omega_f & \Delta\Omega & \Omega_g \end{bmatrix} \tag{B2}$$

and the fact that $k+k'$ is always even. Note that using Eq. (6) with case (a) wave functions, we obtain the same expression for the RLA tensor.

For the b-a CCS, where the ground state belongs to case (b) and the excited state to case (a), we obtain

$$\Theta_{kk'}^{(L)}(\text{b-a}) = (2L+1)(2J_g+1)(2J_f+1)^2(2N_g+1) \begin{bmatrix} J_g & S & N_g \\ \Lambda_g+\Sigma & -\Sigma & -\Lambda_g \end{bmatrix}^2 \begin{bmatrix} J_f & 0 & J_f \\ -\Omega_f & 0 & \Omega_f \end{bmatrix} \times \begin{bmatrix} J_f & L & J_f \\ -\Omega_f & 0 & \Omega_f \end{bmatrix} \begin{bmatrix} J_g & k & J_f \\ \Lambda_g+\Sigma & \Delta\Lambda & -\Omega_f \end{bmatrix} \begin{bmatrix} J_g & k' & J_f \\ \Lambda_g+\Sigma & \Delta\Lambda & -\Omega_f \end{bmatrix}. \tag{B3}$$

Here again, if we set $S=0$ and replace Λ by Ω we obtain the a-a CCS. The RLA tensor for the a-b CCS is given by

$$\Theta^{(L)}_{kk'}(\text{a-b})=(2L+1)(2J_g+1)(2J_f+1)^2(2N_f+1)\begin{Bmatrix} J_f & S & N_f \\ \Lambda_f+\Sigma & -\Sigma & -\Lambda_f \end{Bmatrix}^2\begin{Bmatrix} J_f & 0 & J_f \\ -\Lambda_f-\Sigma & 0 & \Lambda_f+\Sigma \end{Bmatrix}$$
$$\times\begin{Bmatrix} J_f & L & J_f \\ -\Lambda_f-\Sigma & 0 & \Lambda_f+\Sigma \end{Bmatrix}\begin{Bmatrix} J_g & k & J_f \\ \Omega_g & \Delta\Lambda & -\Lambda_f-\Sigma \end{Bmatrix}\begin{Bmatrix} J_g & k' & J_f \\ \Omega_g & \Delta\Lambda & -\Lambda_f-\Sigma \end{Bmatrix}. \tag{B4}$$

We may see from Eqs. (B1), (B3), (B4), and (14) that the isotropic tensor component $\Theta^{(0)}_{kk'}\mathcal{C}$ is identical to the rotational line factor of the corresponding CCS.

If any of the two states has a spin angular momentum S tied to the internuclear axis, its projection is well defined, as is the projection of the electronic orbital angular momentum. Then the angular dependence and the rotational line factor split into two distinct parts and this leads to a simple expression for the angular distribution of the internuclear axis.

For the a-a, a-b, or b-a coupling case sequence we may write

$$\Theta^{(L)}_{kk'}\mathcal{C}=(2L+1)(2J_f+1)\begin{Bmatrix} J_f & 0 & J_f \\ -\Lambda_f-\Sigma & 0 & \Lambda_f+\Sigma \end{Bmatrix}\begin{Bmatrix} J_f & L & J_f \\ -\Lambda_f-\Sigma & 0 & \Lambda_f+\Sigma \end{Bmatrix}\Theta^{(0)}_{kk'}\mathcal{C}\,. \tag{B5}$$

This will not be the case when both the ground and excited state belong to case (b) coupling. In this limiting case, with increasing rotation the spin angular momentum uncouples from the internuclear axis and recouples to N_g to give the resultant total angular momentum J_g. Since the projection of the spin angular momentum on the internuclear axis is not defined, all N_g' which couple to S and have the same projection Λ_g to the internuclear axis leading to the same resultant J_g must be taken into account, as can be seen from Eq. (14). Only for the particular case of singlet transitions can the tensor $\Theta^{(L)}_{kk'}$(b-b), be a factor as in Eq. (B5).

[1] K. H. Kramer and R. B. Bernstein, J. Chem. Phys. **42**, 767 (1965); P. R. Brooks and E. M. Jones, *ibid.* **45**, 3449 (1966); P. R. Brooks, Science **193**, 11 (1976); G. Marcelin and P. R. Brooks, J. Am. Chem. Soc. **95**, 7885 (1973); S. Stolte and B. Bunsengens, Phys. Chem. **86**, 413 (1982).

[2] R. J. Beuhler, Jr. and R. B. Bernstein, J. Chem. Phys. **51**, 5305 (1969); S. L. Anderson, P. R. Brooks, J. D. Fite, and O. V. Nguyen, *ibid.* **72**, 6521 (1980); R. E. Drullinger and R. N. Zare, *ibid.* **51**, 5532 (1969); **59**, 4245 (1973).

[3] D. Van den Ende and S. Stolte, Chem. Phys. Lett. **76**, 13 (1980); Chem. Phys. **89**, 121 (1984).

[4] C. H. Greene and R. N. Zare, Annu. Rev. Phys. Chem. **33**, 119 (1982); J. P. Booth, S. L. Bragg, and G. Hancock, Chem. Phys. Lett. **113**, 509 (1985); W. J. Kessler and E. D. Poliakoff, J. Chem. Phys. **84**, 3647 (1986); R. L. Dubs, S. N. Dixit, and V. McKoy, *ibid.* **85**, 6267 (1986); A. C. Kummel, G. O. Sitz, and R. N. Zare, *ibid.* **88**, 7357 (1988).

[5] R. G. Bray, R. M. Hochstrasser, and H. N. Sung, Chem. Phys. Lett. **33**, 1 (1975); J. R. Lombardi, R. Wallenstein, T. W. Hänsch, and D. M. Friedrich, J. Chem. Phys. **65**, 2357 (1976); J. B. Halperin, H. Zacharias, and R. Wallenstein, J. Mol. Spectrosc. **79**, 1 (1980); K. P. Gros and R. L. McKenzie, J. Chem. Phys. **76**, 5260 (1982).

[6] H. Bebb and A. Gold, Phys. Rev. **143**, 1 (1966); W. Heitler, *The Quantum Theory of Radiation* (Oxford University Press, London, 1954).

[7] M. Born and R. Oppenheimer, Ann. Phys. (Leipzig) **84**, 457 (1927).

[8] J. T. Hougen, *The calculation of Rotational Energy Levels and Rotational Line Intensities in Diatomic Molecules*, Natl. Bur. Stand. (U.S.) Monograph 115 (U.S. GPO, Washington, DC, 1970).

[9] A. R. Edmonds, *Angular Momentum in Quantum Mechanics* (Princeton Unviersity Press, Princeton, 1960).

[10] (a) C. Maínos, Phys. Rev. A **48**, 3242 (1993). (b) The summation over the Euler angles having been performed the normalization factor $(1/8\pi^2)^{1/2}$ is absent from the expression of the rotational wave function, e.g., in case *a* we write $g''=(2J_g+1)^{1/2}\mathcal{D}^{(J_g)*}_{M_g\Omega_g}(\alpha\beta\gamma)$.

[11] C. Maínos, Y. Le Duff, and E. Boursey, Mol. Phys. **56**, 1165 (1985).

[12] J. M. Brown and B. J. Howard, Mol. Phys. **31**, 1517 (1976).

[13] C. Maínos, M. C. Castex, and H. Nkwawo, J. Chem. Phys. **93**, 5370 (1990).

[14] G. Herzberg, *Spectra of Diatomic Molecules* (Van Nostrand, Princeton, 1957).

[15] C. Maínos, Phys. Rev. A **33**, 3983 (1986).

[16] This will also be the case if a single CAM vector is allowed, i.e., for the circular polarization and for the four extreme rotational branches in linear polarization only the $k=n$ value is allowed.

[17] (a) We use the closure relations

$$\sum_{J_f}(2J_f+1)^2(2N_g+1)^2\begin{Bmatrix} N_f & S & J_f \\ k & J_g & J_f \\ N_g & N_g & 0 \end{Bmatrix}^2=1\,,$$
$$\sum_{N_f}(2N_f+1)\begin{Bmatrix} N_g & k & N_f \\ \Lambda_g & \Delta\Lambda & -\Lambda_f \end{Bmatrix}^2=1\,.$$

(b) In circular polarization we have the n-photon angular momentum ($k=n$) collinear ($p=1$) or anticollinear ($p=1$) to the laser beam. In linear polarization we may decompose the incident radiation in left and right circularly polarized components obtaining unit angular momenta collinear or anticollinear to the laser beam; we then obtain $k=n, n-2, \ldots$, which are also aligned along the laser beam. (c) The orientation of the internuclear axis in the excited state may be defined by the vector $\boldsymbol{\Omega}_f=\Omega_f\mathbf{e}_{AB}$ with $\mathbf{e}_{AB}$ a unit vector oriented from the atom A to the atom B in the A-B molecule, $\beta=0$ being associated with $\boldsymbol{\Omega}_f$ collinear and $\beta=\pi$ anticollinear to the polarization vector.

[18] J. R. Appling, M. G. White, T. M. Orlando, and S. L. An-

derson, J. Chem. Phys. **85**, 6803 (1986); R. L. Dubs, S. N. Dixit, and V. McKoy, Phys. Rev. Lett. **54**, 1249 (1985).
[19] F. H. M. Faisal, R. Wallenstein, and H. Zacharias, Phys. Rev. Lett. **39**, 1138 (1977).
[20] S. T. Pratt, E. D. Poliakoff, P. M. Dehmer, and J. L. Dehmer, J. Chem. Phys. **78**, 65 (1983).
[21] S. T. Pratt, P. M. Dehmer, and J. L. Dehmer, Chem. Phys. Lett. **105**, 28 (1984).
[22] P. Baltzer, L. Karlson, and B. Wannberg, Phys. Rev. A **46**, 15 (1992).
[23] F. Merkt and T. P. Softley, Phys. Rev. A **46**, 302 (1992).
[24] (a) M. G. White, W. A. Chupka, M. Seaver, A. Woodward, and S. D. Colson, J. Chem. Phys. **80**, 687 (1984). (b) The photoelectron angular distribution is sharper than the internuclear axis angular distribution in the intermediate excited state and this suggests that there is further selection from the ionization step.
[25] W. J. Kessler and E. D. Poliakoff, J. Chem. Phys. **84**, 3647 (1986).
[26] G. Loge, J. Tiee, and F. B. Wampler, J. Chem. Phys. **79**, 196 (1983).
[27] R. A. Bernheim, C. Kittrel, and D. K. Veirs, Chem. Phys. Lett. **51**, 325 (1977).
[28] S. V. Filseth, R. Wallenstein, and H. Zacharias, Opt. Commun. **23**, 231 (1977).
[29] S. T. Pratt, P. Dehmer, and J. L. Dehmer, J. Chem. Phys. **79**, 3234 (1983).
[30] S. T. Pratt, P. Dehmer, and J. L. Dehmer, J. Chem. Phys. **78**, 4315 (1983).
[31] R. N. Zare, *Angular Momentum, Understanding Spatial Aspects in Chemistry and Physics* (Wiley, New York, 1986).
[32] S. E. Choi and R. B. Bernstein, J. Chem. Phys. **85**, 150 (1986); S. Kaesdorf, G. Schönhense, and U. Heinzmann, Phys. Rev. Lett. **54**, 885 (1985); D. Van den Ende and S. Stolte, Chem. Phys. Lett. **76**, 13 (1980).
[33] This takes place when

$$\begin{Bmatrix} k & L & k \\ 0 & 0 & 0 \end{Bmatrix} \begin{Bmatrix} k & k & L \\ J_f & 0 & J_f \\ J_g & k & J_f \end{Bmatrix}$$

vanishes for any $k = n, n-2, \ldots$ and $L \geq 1$. For instance, this is the case for one-photon transitions with $J_f = \frac{1}{2}$ since in linear polarization only the even values of L are allowed.
[34] This diminution is illustrated by Figs. 2(a) and 2(c) and it is due to the fact that with increasing J_g new M channels are allowed to take place.